HHS Public Access

Author manuscript

J Comp Neurol. Author manuscript; available in PMC 2018 March 21.

Published in final edited form as:

J Comp Neurol. 2008 October 01; 510(4): 396–421. doi:10.1002/cne.21809.

Morphological Analysis of the Mormyrid Cerebellum using immunohistochemistry with Emphasis on the Unusual Neuronal Organization of the Valvula

JOHANNES MEEK, **JIANJI Y. YANG**, **VICTOR Z. HAN**, and **CURTIS C. BELL**

Neurological Sciences Institute and Oregon National Primate Research Center, Oregon Health and Sciences University, Beaverton, Oregon 97006

Abstract

This study used immunohistochemistry, Golgi impregnation and electron microscopy to examine the circuitry of the cerebellum of mormyrid fish. We used antibodies against the following antigens: the neurotransmitters glutamate and γ-aminobutyric acid (GABA); the GABA synthesizing enzyme glutamic acid decarboxylase (GAD); GABA transporter 1; the anchoring protein for GABA and glycine receptors, gephyrin; the calcium binding proteins calbindin and calretinin; the NR1 subunit of the N-methyl-D-aspartate glutamate receptor; the metabotropic glutamate receptors mGluR1α and mGluR2/3; the intracellular signaling molecules calcineurin and calcium calmodulin kinase IIα (CAMKIIα); and the receptor for inositol triphosphate (IP3RIα). Purkinje cells are immunoreactive to anti-IP3R1α, anti-calcineurin and anti-mGluR1α. Cerebellar efferent cells (eurydendroid cells) are anti-calretinin- and anti-NR1-positive in the valvula, but not in the corpus and caudal lobe. In contrast, climbing fibers are anti-calretinin- and anti-NR1- immunopositive in the corpus and caudal lobe, but not in the valvula. Purkinje cells, Golgi cells and stellate cells are GABA positive, whereas efferent cells are glutamate positive. Unipolar brush cells are immunoreactive to anti-mGluR2/3, anti-calretinin and anti-calbindin.

We describe a “new” cell type in the mormyrid valvula, the deep stellate cell. These cells are GABA-, calretinin- and calbindin-positive. They are different from superficial stellate cells in having myelinated axons that terminate massively with GAD- and gephyrin positive terminals on the cell bodies and proximal dendrites of efferent cells. We discuss how the valvula specializations described here may act in concert with the palisade pattern of Purkinje cell dendrites to analyze spatio-temporal patterns of parallel fiber activity.

Keywords

Purkinje cell; climbing fiber; stellate cell; unipolar brush cell; eurydendroid cell; efferent cerebellar neuron; molecular layer; weakly electric fish; Gnathonemus petersii

The cerebellum is one of the most thoroughly studied parts of the vertebrate brain. The orthogonal organization of the transversely running parallel fibers and the sagittally oriented

Correspondence authors: Johannes Meek, Email: hans.meek@hetnet.nl, Victor Z. Han, Oregon National Primate Research Center, Oregon Health and Science University, 505 NW 185th Avenue, Beaverton, OR 97006, Tel: 503 614 3722, Fax: 503 533 2494, Email: Hanv@ohsu.edu.

Purkinje cells has intrigued brain investigators since Cajal (Ramon y Cajal, 1911). The same holds for the interactions between parallel fiber and climbing fiber inputs to individual Purkinje cells (Ito, 1984). The orthogonal organization of the cerebellum has been correlated with precise timing functions (Braitenberg, 1967; Braitenberg et al., 1997; Meek, 1992b; 1997), whereas the interaction between climbing fiber and parallel fiber inputs is thought to mediate synaptic plasticity and have a crucial role in motor learning (Ito, 1984).

Most knowledge about cerebellar mechanisms and function has been obtained in mammals, but comparative brain research has yielded additional information and complementary views. The cerebella of other vertebrates show marked differences and specializations compared to mammals (Larsell, 1967; Nieuwenhuys, 1967; Nieuwenhuys et al., 1997). An exploration of variations in cerebellar organization encountered in vertebrates might help to distinguish between basic cerebellar aspects, encountered in all vertebrate cerebellums, and specializations that are added on to this basic circuitry and function. In this respect, the cerebellum of teleosts is of particular interest. These bony fishes all have a relatively large and well differentiated cerebellum, with some striking differences compared with mammals, to be summarized in the Results section (for reviews, see Finger, 1983; Meek, 1992a; Meek and Nieuwenhuys, 1997). Teleostean cerebellar differentiation and specialization reaches its climax in mormyrid fishes. For instance, the cerebellum of the mormyrid fish *Gnathonemus petersii* encompasses more than half of the total brain and more than one percent of the total body weight (Fig.1; Meek and Nieuwenhuys, 1991; Nilsson, 1996), proportions that are much larger than those found in any mammal.

The molecular layer of the mormyrid cerebellum is more regularly organized and shows different topological arrangements from those found in mammals. The dendrites of most Purkinje cells are arranged in a palisade pattern, meaning that they all are oriented parallel to each other and perpendicular to the cerebellar suface (Nieuwenhuys and Nicholson, 1969b; Meek and Nieuwenhuys, 1991; Han et al., 2006). The distal or ridged part of the valvula of the mormyrid cerebellum shows a number of topological transformations, resulting in a changed location of the molecular layer with respect to the granular layer (Fig. 2; Nieuwenhuys and Nicholson, 1969a; Meek, 1992b).

Mormyrids have an active electrosensory system that includes several specialized brain regions (Bell and Szabo, 1986; Bell, 1986; Meek et al., 1999). These specialized brain regions include a cerebellum-like structure, the electrosensory lateral line lobe (ELL), and parts of the cerebellum itself (Bell et al., 1997, 2005, 2008; Bell, 2002; Meek et al., 1999, 2001, 2004; Zhang et al., 2007). Two regions of the cerebellum are clearly associated with the electrosense: the caudal cerebellar lobe and the mediodorsal region of the distal valvula. The caudal cerebellar lobe is structurally and functionally closely related with the electrosensory lobe (ELL; Campbell et al., 2007). The mediodorsal region of the distal valvula receives a tertiary electrosensory projection from the lateral toral nucleus in the midbrain, which is the main target of the ELL (Finger et al., 1981). The central cerebellar lobes C1, C2, C3, and C4, however, receive little if any electrosensory input (Meek et al., 1986a,b), and the input to most of the valvula is still unknown. So, the specialized cerebellum of mormyrids is only partly, and not exclusively, involved in electroreception. This is in accord with the observation that gymnotid fishes, which also have active

electrosensory systems, do not have an especially large or regular cerebellum (Carr and Maler, 1986).

Several aspects of the so called mormyrid gigantocerebellum (Stendell, 1914; Nieuwenhuys and Nicholson, 1967, 1969a) have been studied, including: connections of different subdivisions (Finger et al. 1981; Bell et al., 1981; Meek et al., 1986a, b); morphology of cerebellar cell types in different subdivisions (Nieuwenhuys and Nicholson 1969b; Nieuwenhuys et al., 1974; Meek and Nieuwenhuys, 1991; Han et al., 2006; Campbell et al., 2007); electron microscopic characteristics of the synaptic organization (Kaiserman-Abramof and Palay, 1969; Meek and Nieuwenhuys, 1991); distribution of Zebrin II (Meek et al., 1992); electrophysiological characteristics of mormyrid cerebellar neurons (Han and Bell, 2003); and plasticity at the parallel fiber to Purkinje cell synapse (Han et al., 2007). From these studies, the basic neuronal organization of the central lobes C1 - C4 (Nieuwenhuys et al., 1974; Meek and Nieuwenhuys, 1991; Han et al., 2006) and of the caudal lobe (Campbell et al., 2007) have become clear. However, data on the intrinsic organization and circuitry of the largest, most distinct and most intriguing part of the mormyrid cerebellum, the distal or ridged valvula, are still fragmentary (Nieuwenhuys and Nicholson, 1969a, b; Kaiserman-Abramof and Palay, 1969).

The present paper uses immunohistochemical techniques to describe and characterize the mormyrid cerebellum, focusing on the histological organization of the valvula cerebelli and a comparison of this organization with that of the corpus and caudal lobe. This immunohistochemical approach turned out to be powerful, since the antibodies selected stained specific cell types reliably in different cerebellar subdivisions. This established a firm base for an identification and comparison of cell types in different subdivisions. Our results also demonstrate the presence of a hitherto unrecognized type of stellate cell in the valvula, referred to here as “the deep stellate cell”. This cell is numerous, morphologically distinct from other stellate cells, and projects to the efferent cells of the valvula. Finally, the present paper presents new data on the distribution of unipolar brush cells and Golgi cells in the granular layer of the mormyrid cerebellum. The dendritic, axonal and basic physiological properties of valvular neurons will be described more completely in an accompanying study by Shi et al. (2008) based on intracellular recording and labeling of cells in brain slices. A short introduction of the teleostean and mormyrid cerebellar organization and subdivisions is presented in the following paragraphs.

Teleostean and mormyrid cerebellar organization

The teleost cerebellum consists of three main subdivisions known, from caudal to rostral as the caudal lobe, the corpus, and the valvula (Figs. 2 & 3). The caudal lobe is considered comparable and probably homologous to the mammalian vestibulo-cerebellum, and the teleostean corpus is homologous to the rest of the mammalian cerebellum. The valvula is a specialization encountered only in actinopterygian fishes, including teleosts, and has no equivalent in mammals. Basically, it is a rostral extension of the cerebellum that protrudes into the midbrain ventricle under the midbrain tectum (see Meek, 1992a, b; Meek and Nieuwenhuys, 1992, 1997).

The intrinsic structure and organization of the corpus cerebelli of teleosts is similar to that of mammals in several respects (compare figs. 12 A and B), including: 1) the presence of three layers, a molecular layer, ganglionic or Purkinje cell layer, and a granular layer; 2) the processing of excitatory mossy fiber input by granule cells and their excitatory parallel fiber projections to the sagittally oriented spiny dendritic tree of Purkinje cells in the molecular layer; 3) an inhibitory projection of Purkinje cells to excitatory efferent cerebellar neurons; 4) the presence of at least two inhibitory interneurons, the Golgi cells of the granular layer and the stellate cells of the molecular layer; and 5) the presence of a sagittally organized olivocerebellar climbing fiber projection to Purkinje cells, which is very specific since each Purkinje cell receives input from only a single climbing fiber.

The most striking difference between the teleostean and mammalian cerebellar organization is the fact that the majority of extrinsic cerebellar projections do not originate from deep cerebellar nuclei, but arise instead from so called eurydendroid or efferent cells, which have their soma in the same layer as Purkinje cells (Fig. 12B; Nieuwenhuys et al., 1974; Finger, 1978, 1983; Murakami and Morita, 1987; Meek and Nieuwenhuys, 1997). Since this layer contains both Purkinje cells and efferent cells, it is referred to as the ganglionic layer, rather than the Purkinje cell layer. Teleostean cerebellar efferent cells have non-spiny dendrites in the molecular layer that receive parallel fiber input, a remarkable difference from the deep cerebellar nucleus neurons of mammals that receive most of their excitatory input from mossy fibers. The axons of efferent cells leave the cerebellum unbranched, without intracerebellar collaterals. Because of the location of efferent cells within the ganglionic layer, most Purkinje cells are interneurons with axons that stay and terminate within the ganglionic layer and do not penetrate the granular layer to terminate on deep cerebellar projection neurons, as mammalian Purkinje cell axons do.

A second difference between the teleostan and mammalian cerebellar organization is the fact that olivocerebellar “climbing” fibers do not “climb” into the molecular layer. In teleosts, their terminals are restricted to the ganglionic layer, where they synapse upon the proximal dendrites and cell bodies of Purkinje cells (Pouwels, 1978; Meek and Nieuwenhuys, 1991; Han et al., 2006; Shi et al. 2008). A third difference is that basket cells are absent in teleosts (compare figs. 12A and B). A fourth and final difference is that many mossy fibers in teleosts originate from a special mesencephalic precerebellar nucleus located at the rostral base of the cerebellum (the nucleus lateralis valvulae), which has no homologue in mammals (Ito and Yoshimoto, 1990; Meek et al., 1986a,b; Meek, 1992a; Meek and Nieuwenhuys, 1997).

On top of the differences just enumerated, mormyrids show the following additional specializations compared with mammals as well as other teleosts: 1) the dendrites of the Purkinje cells form a palisade pattern in the molecular layer (Nieuwenhuys and Nicholson, 1969b; Meek and Nieuwenhuys, 1991; Han et al., 2006); 2) the valvula is very large and has reached a location dorsal to all other parts of the brain by pushing the midbrain tectum aside (Fig. 2A,B,C; Nieuwenhuys and Nicholson, 1967, 1969a); 3) the valvula shows several topological transformations, as a result of which the location of the granular cell layer with respect to the molecular and ganglionic layers (which maintain their mutual relationships in all valvular subdivisions) changes from caudal to rostral (Fig. 2 D,E,F; Nieuwenhuys and

Nicholson, 1969a); and 4) in the caudal lobe of mormyrids Purkinje cells are not located in a layer, but “invade” the molecular layer, where they are more or less randomly distributed (Campbell et al., 2007). Mormyrids share the latter feature with the caudal lobes of some, but probably not all teleosts (Meek and Nieuwenhuys, 1997)

Mormyrid cerebellar subdivisions

The caudal lobe of mormyrids, including *Gnathonemus petersii*, consists of two main subdivisions, the anterior and the posterior caudal lobe (LCa and LCp, respectively). Each subdivision can be further subdivided into a dorsal and a ventral part (Fig. 3). The caudal lobe is related to the eminentia granularis, which consists of granule cells that give rise to the parallel fibers of the caudal lobe, and can be similarly subdivided into an anterior and posterior part (EGa and EGp respectively), related to LCa and LCp respectively. EGa gives rise not only to the parallel fibers of the caudal lobe, oriented transversely, but also to the parallel fibers of the cerebellar crest, which run rostro-caudally. EGp sends parallel fiber projections to both LCp and the electrosensory lateral line lobe (ELL). Both populations of parallel fibers run transversely (Meek 1992b; Campbell et al. 2007). Most likely, the projections to LCa and LCp originate from the dorsal portions of EGa and EGp, respectively, whereas the projections to the cerebellar crest and ELL probably originate from the ventral subdivisions of EGa and EGp, respectively, but this has not been established with certainty.

Rostral to the caudal lobe, four lobes can be distinguished in sagittal sections, indicated from rostral to caudal as lobe C1 to C4 (Fig. 3a). We will maintain this widely adopted nomenclature, but it should be made clear that we consider only lobe C4, lobe C3 and the dorsal part of lobe C2 (C2d) as **the corpus cerebelli**. Previous studies confusingly included all central lobes in the corpus. However, Meek et al. (1992) and Meek (1992b) concluded on the basis of Zebrin II immunochemistry and obvious morphological differences that lobe C1 and the ventral part of lobe C2 form a rostocaudally folded continuous sheet of cerebellar tissue that is part of the valvula and not the corpus. Our present immunohistochemical data strongly support this conclusion. In lobes C3 and C4, rostral, caudal, dorsal, ventral and lateral parts may be distinguished (Fig 3).

The valvula of *Gnathonemus* may be subdivided into a proximal and a distal valvula. The proximal valvula consists of the ventral part of lobe C2, lobe C1 and the lobus transitorius (LT). Lobe C1 can be subdivided on the basis of its major folds into a caudal, dorsal and rostral part (Fig. 3a). The distal valvula is by far the largest part of the mormyrid cerebellum (Figs. 1, 2) and consists of a huge plate of granule cells, covered with ridges of molecular and ganglionic layer, oriented perpendicularly to the granular layer (Fig. 2F; Nieuwenhuys and Nicholson, 1969a). Therefore, we will also refer to this part of the valvula as the ridged valvula. In the ridged valvula, parallel fibers enter the molecular layer from only one side without bifurcation (Fig. 2F); in the lobus transitorius, parallel fibers enter the molecular layer from two sides without bifurcation (Fig. 2E), and in lobe C1 the latter configuration is combined with the more general and well known origin of parallel fibers by bifurcation from ascending branches of granule cell axons (Fig. 2D; Meek 1992b). In the ridged valvula, the

major efferent cells are located at the base of the ridges (Fig. 2F) and are referred to as basal cells, following Nieuwenhuys and Nicholson (1969a,b).

MATERIALS AND METHODS

General Procedures

The present study is based on the same material and sections as our previous study on the immunocytochemical identification of cell types in the mormyrid electrosensory lobe (Bell, et al., 2005). For details, the reader is referred to the methods section of that paper (Bell et al., 2005). All the fish used in this study were of the mormyrid species *Gnathonemus petersii*. The Institutional Animal Care and Use Committee of Oregon Health and Sciences University approved the procedures.

The histological procedure was as follows: Fish were deeply anesthetized in cold tricaine methane sulfonate (MS-222, 1:10,000) before being perfused through the heart with 0.7% NaCl followed by perfusion with a fixative. The fixative in most cases was 4 % paraformaldehyde in 0.1 M phosphate buffer (PB), except for the antibodies to GABA and glutamate. Since the antibodies used to localize GABA and glutamate are in fact antibodies to the glutaraldehyde conjugates of these amino acids, the fixative used for tissue to be treated with these antibodies was 2% paraformaldehyde and 2% glutaraldehyde in PB. Brains were postfixed with the same fixative with which they were perfused. Fifty micron transverse sections were cut with a vibratome and all subsequent reactions were done with free floating vibratome sections.

The general immunocytochemical protocol was:

1. Four 10 minute washes in PB (pH 7.4 in all procedures).
2. Blocking for 2 hours with different blocking solution (see below for specific data per antibody).
3. Reaction with primary antibody in the same blocking agent as used in step 2. All primary antibodies were made in rabbits, except for the gephyrin antibody which was made in mouse.
4. Four 10 minute washes in PB.
5. Reaction with secondary antibody for 4 hours in the same blocking agent as used in steps 2 and 3. With most primary antibodies the secondary antibody was a goat anti-rabbit IgG (Vector, Burlingame, CA) at a concentration of 1:200. With the anti-gephyrin antibody the secondary was a goat anti-mouse IgG (Vector) at a concentration of 1:200.
6. ABC (Vector) in PB overnight.
7. Five 10 minutes washes in PB.
8. Reaction with diamino-benzidine (DAB; 10 mg/20 ml PB) for 30 minutes.
9. Reaction with DAB in above solution plus 5μl 3% hydrogen peroxide for 5 - 15 minutes.

10. Three 10-minute washes in PB.

11. Mounting of sections on slides and coverslipping.

Control procedures in which primary antibody was omitted and in which secondary antibody was omitted were carried out with each antibody, with all other aspects of the procedures being the same. These controls showed no cell-specific staining. Several antibodies from Chemicon were used. Except where noted, these same antibodies are now available through Millipore which has retained the same numbering system that was used by Chemicon.

Antibody specific procedures

Calbindin—The antibody was kindly provided by Dr. Kenneth Baimbridge of the University of British Columbia. The antibody (Dr. Baimbridge's number 8701) was made against bovine brain calbindin (Conde et al. 1994). Dr. Baimbridge showed that this antibody labels a single 28Kd protein band on Western blots of tissue from rat cerebellum and does not cross react with calretinin or other proteins at normal working dilutions. Immunoprecipitation of rat cerbellar soluble proteins with this antibody followed by protein agarose gel electrophoresis (PAGE) also yielded a single 28Kd band (personal communications from Dr. Kenneth Baimbridge). A previous study in our laboratory on the mormyrid electrosensory lobe used the same antibody and showed that it stains a 28Kd protein on Western blots of both mormyrid brain and rat cerebellum (Bell et al. 2005). We also tested this antibody on rat cerebellar tissue and found that it stains Purkinje cell somas and dendrites in a manner that appeared completely similar to the staining pattern described for other anti-calbindin antibodies (Baimbridge and Miller 1982; Bastianelli 2003) The blocking solution was 10% normal goat serum (Vector) with 0.5% Triton in 0.1% PB. Sections were soaked in the primary antibody at a concentration of 1:1,500 for 20 hours at room temperature.

Calcineurin—The calcineurin antibody (Chemicon, Temecula, CA, #AB1694) was a polyclonal against purified bovine brain calcineurin. According to the manufacturer, this antibody recognizes both the catalytic A and regulatory B subunits of calcineurin, a calcium- and calmodulin-dependent protein phosphatase. The antibody was affinity purified. This antibody labels bands on Western blots of homogenates of mouse cardiac tissue at the molecular weights of the A and B subunits of calcineurin, but does not label other bands (Bueno et al. 2002). This antibody stained all Purkinje cells in the mormyrid cerebellum in a manner similar to that observed with the same antibody in mammalian Purkinje cells (Usuda et al. 1996). The blocking solution was 5% nonfat dry milk in 0.3% triton in 0.1M PB. Sections were soaked in the primary antibody at a concentration of 1:200 for 40 hrs at 4° C.

Calretinin—The antibody was kindly provided by Dr. John Rogers of Cambridge University. The antibody was made against a beta-galactosidase-calretinin fusion protein containing putative calcium binding domains III-IV (Rogers, 1989). The calretinin was from chick. Our previous study, using this same antibody, showed in Western blots that it stains a single 29 Kd band in rat brain homogenates and a single, 28kD, band in mormyrid brain homogenates that is presumed to be a slightly different form of calretinin (Bell et al. 2005). See Bell et al. (2005) for discussion of this small difference in molecular weight. The

molecular weights of the proteins stained with the calbindin and calretinin antibodies were similar. However, as described in the previous study by Bell et al. (2005) and in this one, the immunocytochemical staining patterns using the calbindin and calretinin antibodies were distinct. The blocking solution was 2% bovine serum albumin with 0.5% Triton in 0.1 M PB. Sections were soaked in the primary antibody at a concentration of 1:1250 for 20 hours at room temperature.

Calcium-calmodulin kinase II alpha (CaMKIIα)—The antibody (Boehringer Mannheim, Indianapolis, IN, #1481703) was a monoclonal made against purified rat ***CaMKIIα*** (Erondu and Kennedy, 1985). The ***CaMKIIα*** was purified by the calmodulin-sepharose step as described by Kennedy et al. (1983). Immunoblots with SDS-PAGE show that the antibody reacts with a single 50Kd band in rat brain homogenates. The alpha subunit of CaMKII has a molecular weight of 50 Kd and the band can be removed with a preceding immunoprecipitation with another antibody to the alpha subunit (Erondu and Kennedy 1985). A previous study by Bell et al. (2005) showed that this antibody stains the deep molecular layer of the mormyrid electrosensory lobe where descending fibers from the preeminential nucleus terminate. This pattern of staining is the same as that shown by Maler et al. (1999) in the electrosensory lobe of the gymnotid fish Apteronotus leptorhynchus using the same antibody. The blocking solution was 2% normal goat serum with 0.3% triton in 0.1M PB. Sections were soaked in the primary antibody at a concentration of 1:800 for 20 hours at room temperature.

Gamma Aminobutyric Acid (GABA)—The antibody (Diasorin. Stillwater, MN #20094) was against GABA coupled to bovine serum albumin with glutaraldehyde. The blocking solution was 3% bovine serum albumin with 0.3% Triton in 0.1 M PB. Sections were soaked in the primary antibody at a concentration of 1:16,000 for 20 hours at room temperature.

GABA transporter 1 (GAT-1)—The antibody (Chemicon #AB1570) was a polyclonal made against the C-terminus (amino acids 588-599) of rat GAT-1. The antibody was affinity purified. Specificity of staining was shown by the blocking of immunostaining when the antibody was preabsorbed with the GAT-1 polypeptide but not when it was preabosrbed with GAT-2, GAT-3, or the glycine transporter GLYt-1 (Minelli et al. 1995). The blocking solution was 5% nonfat dry milk with 0.3% Triton in 0.1M PB. Sections were soaked in the primary antibody at a concentration of 1:1000 for 12 hours at room temperature.

Glutamic acid decarboxylase (GAD)—The antibody (Chemicon #AB108) was a polyclonal against GAD 67 derived from cloned feline DNA expressed in E. Coli. (This antibody is no longer available.) Western blots using whole brain homogenates of mouse, rat and human brain showed that this antibody stains a single band at 67Kd (Kaufman et al. 1991). The blocking solution was 10% normal goat serum in 0.1M PB. Sections were soaked in the primary antibody at a concentration of 1:2000 for 20 hours at room temperature.

Gephyrin—The antibody we used was a monoclonal made against purified rat gephyrin. Gephyrin is an oligomer. The antibody binds predominantly to the 93 Kd polypeptide of the extracted oligomer and to a lesser extent to the 48 Kd polypeptide as shown by gel

electrophoresis (Pfeiffer et al. 1984). The antibody binds to the N terminus of the protein. The antibody was originally obtained from Cedarlane Laboratories, Hornby, Ontario, Canada (CL281205030) but they no longer provide it. Antibody from the same clone (mAB7a) is available, however, from Synaptic Systems GMBH (147011(SY)). The blocking solution was 5% nonfat dry milk with 0.3% Triton in 0.1M PB. Sections were soaked in the primary antibody at a concentration of 1:1,000 for 40 hours at 4° C.

Glutamate—The antibody (Biogenesis, Kingston, NH, AR1766) was against glutamate coupled to bovine serum albumin with glutaraldehyde. The blocking solution was 3% bovine serum albumin with 0.3% Triton in 0.1M PB. Sections were soaked in the primary antibody at a concentration of 1:5,000 for 20 hours at room temperature.

Inositol triphosphate receptor I (IP3RI)—Dr. Pietro de Camilli of Yale University kindly provided the antibody (Mignery et al., 1989). The antibody was made against the 19 C-terminal residues of the mouse cerebellar IP3 receptor (amino acid residues 482-500). Western blots of mouse brain tissue showed that the antibody labels a single 260 Kd band, the molecular weight of the mammalian IP3RI protein. Our previous study showed with a Western blot of mormyrid brain that the antibody also stains a single band at 260 Kd, in the mormyrid brain (Bell et al. 2005). All Purkinje cells in the mormyrid brain stain throughout their dendirtic arbors, as in the mammal (Mignery et al. 1989), The blocking solution was 2% nonfat dry milk with 0.3% triton in 0.1M PB. Sections were soaked in the primary antibody at a concentration of 1:500 for 40 hours at 4° C.

Metabotropic glutamate receptor 1 alphã (mGluR1 α)—The antibody (Chemicon, AB1551) was made against a carboxy-terminal peptide of rat mGluR1-conjugated to keyhole limpet hemocyanin (KLH) with glutaraldehyde (PNVTYASVILRDYKQSSSTL). Our previous study, using this same antibody, showed the same staining pattern on Western blots for both rat brain and mormyrid brain homogenates (Bell et al. 2005). The main bands in both species were at two times the molecular weight of the protein reflecting dimerization. The antibody was affinity purified. The blocking solution was 3% bovine serum albumin with 0.3% Triton in 0.1M PB. Sections were soaked in the primary antibody at a concentration of 1:200 for 20 hours at room temperature.

Metabotropic glutamate receptor 2/3(mGluR2/3)—The antibody (Chemicon AB1553) was a polyclonal made against a carboxy-terminus peptide of rat mGluR2 conjugated to bovine serum albumin with glutaraldehyde (NGREVVDSTTSSL). The antibody was affinity purified. Our previous study, using this same antibody, showed the same staining pattern on Western blots for both rat brain and mormyrid brain homogenates (Bell et al. 2005). The main bands in both species were at two times the molecular weight of the receptor protein, reflecting dimerization. The blocking solution was 5% nonfat milk with 0.3% Triton in 0.1M PB. Sections were soaked in primary antibody at a concentration of 1:200 for 20 hours at room temperature.

N-methyl-d-aspartate receptor subunit 1 (NR1)—The antibody was kindly provided by Dr. Robert Dunn of McGill University. The antibody was prepared against a recombinant form of the NR1 subunit (Bottai et al., 1997; Berman et al. 2001) of the South American

electric fish Apteronotus leptorhynchus. The antibody was prepared against a 57 amino acid sequence from the carboxy terminal (amino acids 844-901) of the protein. Western blots in Apteronotus showed that the antibody stained a single band at 110kDa (Berman et al. 2001). The staining pattern in spines of Purkinje-like cells of the electorosensory lobes of mormyrids (Bell et al. 2005) is essentially the same as that in similar cells in the gymnotid fish Apteronotus (Berman et al. 2001). The blocking solution was 10% normal goat serum with 0.3% triton in 0.1M PB. Sections were soaked in primary antibody at a concentration of 1:2000 for 20 hours at room temperature.

Immunospecificity

The immunospecificity of the antibodies that we used against calbindin, calretinin, mGluR1α, mGluR2/3, and IP3R1 was determined with Western blots, as described in a previous study on the mormyrid electrosensory lobe that used the same antibodies (Bell et al. 2005). In that study, we compared the Western blot results for homogenized mormyrid brain tissue with those for homogenized rat brain tissue and found them closely comparable. For both homogenates, the Western blots indicated the specificity of the antibodies, as described in the preceding paragraphs and in the revious study. Our previous study should be consulted for a detailed description of the methods and results of the Western blots using these five antibodies.

The immunospecificity of the antibodies that we used against glutamate, GABA, GAD and GAT-1 was not specifically tested for mormyrid brain tissue with Western blots, since the immunospecificity of these widely applied antibodies could be concluded from comparison with cerebellar results in other vertebrates, including mammals. In all vertebrates, similar excitatory efferent cells (anti-glutamate) or (subparts of) inhibitory GABAergic Purkinje cells, stellate cells and Golgi cells (anti-GABA, anti-GAD and anti-GAT-1) react with these antibodies. The specificity of our anti-gephyrin antibody for postsynaptic specializations of GABAergic and glycinergic synapstic contacts was concluded from the size and distribution of the fine spots labeled (e.g. fig. 9B, D), both in the mormyrid ELL (Bell et al., 2005) and the mormyrid cerebellum, where it corresponds well with the distribution of GAD- and GABA-positive terminals.

We did not have the possibility to test the immunospecificity of the anti-calcineurin, anti-CaMKII and anti-NR1 antibodies used in the present study. So, we can not exclude the possibility that these antibodies might possibly bind in the mormyrid brain to another antigen than the one to which they were raised, and we are presently not sure that staining with these antibodies really indicates the presence of calcineurin, CaMKII and NR1, respectively, in the mormyrid cerebellum. So, we used these antibodies exclusively as anatomical markers for certain cell types, for which purpose they appeared to be as useful as the other antibodies applied in the present study.

Electron microscopy and Golgi impregnation

Some Golgi pictures of (eurydendroid) cerebellar efferent neurons as well as some electron microscopical aspects of their synaptic connections are included in the present paper to complement our immunohistochemical analysis. For this purpose, the same Golgi material

and the same normal, untreated as well as Golgi-(de)impregnated material was analyzed as used for our previous study on the (ultra)structure of cerebellar Purkinje cells (Meek and Nieuwenhuys, 1991), and that paper should be consulted for details concerning the Golgi-rapid procedure and the normal and Golgi-EM techniques applied.

Estimation of relative numbers, sizes and shapes of cells types

We obtained rough estimates of the relative numbers of different cerebellar cell types in distinct cerebellar subdivisions by counting the numbers of cells stained by the best antibody for each cell type in comparable sagittal and/or transverse sections. For each ratio, the counts in 3 - 5 sections were averaged and then compared.

An estimation of the average sizes and shapes of the cell bodies of different cell types in different subdivisions of the mormyrid cerebellum was obtained by measuring and averaging the largest and smallest diameters of 50 to 100 profiles with a nucleus in sections treated with the best antibody for each cell type.

Photomicrography and figure preparation

Photomicrographs were taken with a digital camera and stored as TIF files. Electron microscopic images were also stored as TIF files. These files were imported into the graphics program Coreldraw 11 (Corel, Ottawa, Canada) for cropping, layout, and lettering. The finished figures were exported from Coreldraw as TIF files.

RESULTS

The present immunohistochemical analysis of the mormyrid cerebellum yielded insight into the distribution, chemical and morphological differentiation of cerebellar neurons in different cerebellar subdivisions. To present our result as clearly as possible, we have summarized the cerebellar neural elements stained by different antibodies in a table and will start with a short survey of the general features of immunohistochemically stained cerebellar cell types. The main part of the results describes the variations in neuronal morphology and circuitry as observed in the corpus, the caudal lobe, the proximal valvula, and the distal (ridged) valvula, respectively. Figure 4 provides a schematic overview. Figure 5 shows details of our results from the corpus, figure 6 from the caudal lobe, figures 7-10 from the proximal valvula, and figure 11 from the ridged valvula.

General features of immunohistochemically stained mormyrid cerebellar elements

Purkinje cells were immunopositive throughout all mormyrid cerebellar subdivisions for anti-IP3R, anti-calcineurin and anti-mGluR1α, which stained both the cell bodies and dendrites quite intensely (Fig. 5 A, B, C). All three antibodies showed the presence of a regular palisade organization of the spiny apical Purkinje dendrites in the molecular layer of the corpus and valvula (Figs. 4A, 5A, 7A) but not in the caudal lobe (Figs 4A; 6A). The thin, sagittally oriented axons of Purkinje cells could be followed over considerable distances in sections treated with anti-IP3R or anti-calcineurin (Figs 5A; 7A). Axon terminals were hardly immunopositive to any of the antibodies mentioned above. However, the gephyrin- and GAD-positive terminals in the ganglionic layer (Figs 5H, 8B; 9B; 11H) probably

include Purkinje axon terminals, as may be inferred from their distribution as described on the basis of Golgi impregnation (Meek and Nieuwenhuys, 1991) and intacellular labeling (Shi et al. 2008). Purkinje cell bodies and proximal dendrites were faintly but clearly GABA immunoreactive. However, the distal, spiny palisade dendrites in the molecular layer were hardly stained by anti-GABA in our material (Figs 5G; 8C; 11F).

Anti-IP3R, anti-calcineurin and anti-mGluR1α staining resembles Zebrin II staining of Purkinje cells as described previously (Meek et al. 1992; Campbell et al. 2007), with the exception that all Purkinje cells are stained by anti-IP3R, anti-calcineurin and anti-mGluR1α, whereas Zebrin II left some populations unstained. Staining of Purkinje cell axons with antibodies to IP3R (present study) and to Zebrin (unpublished observations) stain terminals of Purkinje cells in brainstem vestibular nuclei that arise from a subset of Purkinje cells in the caudal lobe, as has also been described in other teleosts (Brochu et al., 1990). Purkinje cells in all other parts of the mormyrid cerebellum appear to be interneurons with axons restricted to the cortex.

Efferent cerebellar neurons were immunopositive to anti-NR1 and anti-calretinin in both the proximal and the ridged valvula (Figs. 7B, C; 9A; 11C, G). Valvular efferent cells were also positive to anti-glutamate (Fig. 8A, 11E) and were densely covered with gephyrin-, GAD- and GABA- positive terminals (Figs. 8B, C; 9B-D; 11F, H). Valvular efferent cells were either not labeled or only faintly labeled with the anti-calbindin antibody (Figs. 7D; 11B), except for a few ridges in the ventrolateral valvula (see discussion for possible reasons).

In the corpus and caudal lobe, efferent cells were not NR1-, calbindin- or calretinin-positive, with an exception in the caudal part of C4 (Fig 4C, D; see below). Only a few efferent cells in the corpus displayed clear glutamate immunoreactivity (Fig. 5F). Because of the absence of distinct immunolabeling of efferent cells in the corpus, we included some Golgi and EM observations on these neurons in the present study to describe their morphology and their place in cerebellar circuitry below.

Stellate cells were immunoreactive to GABA throughout the cerebellum (Fig. 4D). In both the proximal and ridged valvula, they appear to be concentrated in a particular sublayer between the lower molecular layer and the ganglionic layer (Figs. 8C, 11F). This numerically large population appears also to be strongly immunoreactive to both anti-calbindin and anti-calretinin (Figs. 7B-D; 9A; 11B, C, G) and weakly immunopositive to anti-NR1. We will refer to these neurons as ***deep stellate cells,*** since we consider them as a specialized valvular cell type derived from the more superficially located and smaller, “classical” stellate cells of the valvula. This is based on their common GABAergic nature, calretinin-positivity and dendritic properties (i.e. having non-spiny dendrites in the molecular layer). However, the axonal properties of deep and superficial stellate cells are different (see below).

The small, “classical”, superficial stellate cells are more or less randomly distributed throughout all cerebellar subdivisions and throughout the superficial to deep extent of the molecular layer, including the valvula (Fig. 4D). Immunohistochemistry using anti-GABA

transporter showed a fine but rather dense network of axons and small terminals in the molecular layer, most likely representing the axonal plexus of superficial stellate cells (Fig. 5I, J). This can be concluded from the similar presence of this network in the molecular layer throughout all cerebellar subdivisions. Calbindin and calretinin immunohistochemstry strongly suggest that the axons of deep stellate cells terminate in and around the ganglionic layer, predominantly on efferent valvular cells (see below) but also perhaps on other deep stellate neurons and Purkinje cells.

Golgi cells were GABA immunoreactive throughout all cerebellar subdivisions (Figs. 4D; 5G), and weakly positive to anti-calbindin in a number of our preparations. They have a rather low frequency of occurrence in the mormyrid cerebellum and may be located in the superficial part of the granular layer just below the ganglionic layer, or deep in the granular layer. GAD- immunohistochemistry shows a rather random distribution of GAD-positive terminals in the granular layer, most likely representing the axonal terminals of Golgi cells. This might suggest that mossy fiber glomeruli, around which Golgi axons are concentrated in mammals (Ito, 1984) are smaller in mormyrids that in mammals, similar to reports for trout (Pouwels, 1978) and dogfish (Alvarez-Otero et al., 1995).

Unipolar brush cells (UBC's) were immunoreactive to anti-mGluR2/3, anti-calretinin and anti-calbindin. The latter two antibodies also stain populations of mossy fibers in the granular eminences (see below), so the distribution of UBC's was most clearly demonstrated by mGluR2/3, which did not stain any other element in the granular layer. UBC's in the mormyrid brain are morphologically similar to those in the mammalian brain, with a unipolar cell body slightly larger than the granule cells and a single, short, thick dendrite terminating in a brush-like structure (Jaarsma et al. 1998; Fig 6C, E). The frequency of occurrence of UBC's is quite high in the granular eminences, where they occur throughout the granular layer (Fig. 4B). In the corpus cerebelli (lobes C4 and C3) they are almost exclusively located in the latero-dorsal portion of the granular layer (Fig 5D). In the granular eminences, clusters of gephyrin-positive spots occur with a similar number, density and distribution as that of unipolar brush cells (Fig. 6D). Such clusters were absent in the corpus and valvula, suggesting that they are related to UBC's (see below). Since Golgi cells are the only source of GABAergic synapses in the granular layer, this point to a strong inhibition of UBC's by Golgi cells in the granular eminences.

Remarkably, mGluR2/3-positive UBC-like cells, with a similar unipolar soma and single dendrite terminating in a brush, also occur in the molecular layer of the caudal lobe (Figs. 4B, 6F). We refer to these cells as UBC-*like*, since they are not calretinin or calbindin-positive and since they occur in the molecular layer, where UBC's are not found in mammals and where they must have a different place in cerebellar circuitry. mGluR2/3 positive UBC-like cells that are not calretinin or calbindin positive were also observed at the meningeal boundary region at the base of the granular layer of the ridged valvula (Fig. 4B).

Granule cells and their parallel fibers were not immunoreactive to any of the antibodies used in our material, with the result that the present study unfortunately did not yield further insight in the intriguing origin and topography of parallel fiber projections to the molecular layer in different subdivisions.

Climbing fibers were immunoreactive to anti-calretinin and anti-NR1, but only in the corpus and caudal lobe (Figs. 4C; 5D, E; 6B). Climbing fibers in most of C2v, C1, LT and the valvular ridges were not immunorreactive to any of the antibodies used in our present study. Calretinin-positive climbing fibers, calretinin-positive valvular efferents, and calretinin-positive deep stellate cells coexist within a narrow boundary region between C2d and C2v (Fig. 4C). Examination of this region showed that, at least in this region, climbing fibers do not terminate on efferent cells or on deep stellate cells, but exclusively on Purkinje cells. We presume that this equally holds true for other parts of the cerebellum, as was ascertained with electron microscopy for lobe C3 of the corpus and lobe C1 of the proximal valvula (see below).

Mossy fibers were only stained in substantial numbers in the granular eminences, both by anti-calretinin and anti-calbindin. Anti-calretinin positive fibers in the corpus could usually be identified as passing climbing fibers (Fig. 4 D,E), and in the valvula as axons of deep stellate cells (Figs. 7D; 9A; 11G) or efferent cells (Figs. 7B, 11B,C). However, we cannot exclude the possibility that a few mossy fibers in the corpus and valvula are anti-calretinin- and/or anti-calbindin-positive as well.

egional histological specializations

The corpus cerebelli—With respect to the morphological organization of the cerebellar corpus (lobes C4, C3 and C2d), the present immunohistochemical results (Fig. 5) basically confirmed previous descriptions of this region (Meek and Nieuwenhuys, 1991; Han et al., 2007). Accordingly, Purkinje cells in the corpus are located in the ganglionic layer and have palisade dendrites (Fig. 5A, B, C), while climbing fibers and their terminals are restricted to the ganglionic layer (Fig. 5D,E). The occurrence of unipolar brush cells is largely restricted to the latero-dorsal part of the granular layer (Fig. 5D), with the exception of a few cells located in the midline region (Fig. 4B). Superficial stellate cells are randomly distributed in the molecular layer with a low frequency of occurrence, while deep stellate cells are absent (Figs. 4D, 5G). In spite of their low number, stellate axons establish a quite dense GABA-transporter 1-immunopositive network in the molecular layer (Fig. 5I, J). Golgi cells occur in low numbers throughout the granular layer, with a slight preference for the superficial part just under the ganglionic layer (Figs. 4D, 5G). Mossy fibers and granule cells of the corpus remained unresponsive to the immunohistochemical procedures used in the present study. In material treated with anti-IP3R, Purkinje cell bodies of the corpus have an average size of about 10 × 8 μm. In sections treated with anti-GABA they are slightly larger, i.e. about 11 × 9 μm. In the laterocaudal part of C4 they are significantly larger (IP3R: 16 × 10 μm; GABA: 14 × 10 μm), but in the ventral part of C3 somewhat smaller (IP3R: 8 × 6 μm; GABA: 9 × 8 μm).

Efferent cells in the corpus were not stained in our immunohistochemical material, except for a few glutamate-positive cells that probably are efferent cells (Fig. 5F). Some cells marked by a substantial density of GAD- or gephyrin positive terminals might also represent E-cells. Comparison with their frequency of occurrence in (sagittally sectioned) EM material suggests that probably only a small fraction of efferent cells of the corpus were visualized in our (transversely sectioned) glutamate material. Golgi- and EM observations show that

efferent cells in lobe C3 have sagittally oriented dendritic trees with numerous, thin, non-spiny dendrites in the molecular layer (Fig. 10A). They have a light cytoplasm and receive synaptic contacts from a low to moderate number of axon terminals (Fig. 10F). Some of them could be identified as Purkinje axon terminals on the basis of our previous characterization (Fig. 10D; Meek and Nieuwenhuys, 1991), but another population has a much lighter cytoplasm and resembles the deep stellate axon terminals of the valvula (Fig. 10E, see below). In the caudal region of lobe C4, efferent neurons were immunoreactive to anti-calretinin, similar to the efferent cells in the valvula (Fig. 4C; see below). This immunoresponsiveness was associated with the presence of calbindin- as well as calretinin-positive deep stellate neurons in the same region (Fig 4D). So, the most caudal region of the corpus seems to be distinct from the rest of the corpus and shows several similaries with the organization of the valvula.

The caudal lobe and granular eminences—The present study confirms the organization of this mormyrid cerebellar specialization as recently described by Campbell et al. (2007), and extends their observations with some details on Purkinje cell bodies, climbing fibers, and unipolar brush cells (UBC's; Fig. 6). The most remarkable aspect of the caudal cerebellar lobe of mormyrids is that Purkinje cell bodies and climbing fibers are present in the molecular layer (Fig. 6A, B, F), which is seen nowhere else in the mormyrid cerebellum (Fig 4A, B, C). Climbing fibers have to penetrate the molecular layer (Fig. 6B) in order to innervate the cell bodies and proximal dendrites of Purkinje cells. Caudal lobe Purkinje cells do not show a palisade pattern, and in LCav and LCpv do not even have a clear sagittal orientation of their dendritic tree (Fig. 6A).

Purkinje cell bodies in LCpv, LCpd and LCav of the caudal lobe all measure on average about 16 × 11 μm in sections treated with anti-IP3R, which is substantially larger than in the corpus or valvula. The Purkinje cells in LCad were smaller, i.e. on average about 12 × 10 μm, which is only a little bit larger than in the corpus.

UBC's are quite numerous and widely distributed in both EGa and EGp, as revealed by anti-mGluR2/3-, anti-calretinin- and anti-calbindin immunohistochemistry. They have a small cell body and only one short dendrite that ends in a structure indicated as a brush, but which in our material more resembles a glomerulus (Fig. 6C, E). The axons of UBC's were either not stained or stained for only a short distance in our immunohistochemical material (Fig. 6C), so we could not follow them to possible terminals or glomeruli.

Remarkably, in material treated with anti-mGlur2/3, UBC-like cells were present in the molecular layer of the caudal lobe, with a rather high density in LCp (Figs 4B, 6F). In contrast to the UBC's of EGa and EGp, these "displaced" UBC-like cells were not calretinin- or calbindin-positive. Whether these UBC-like cells are part of the neural circuitry of the LC molecular layer or whether they are immature, migrating cells on their way to the granular eminences, is uncertain. However, their morphology seems quite "adult", and a soma, brush and axon may be identified (Fig. 6F).

Anti-gephyrin immunohistochemistry shows a peculiar clustering of gephyrin-positive postsynaptic spots in the EGa as well as in the EGp, with a similar density and distribution

as UBC's (Fig. 6D). Such clusters of gephyrin-positive spots are absent in other cerebellar regions. This suggests that the brushes and/or the axonal glomeruli of UBC's are especially densely innervated by Golgi axons, the only source of inhibitory axon terminals in the granular layer. It has been demonstrated that mammalian UBC's are glutamatergic, with an axon that makes mossy-fiber like, glomerular, excitatory connections with granule cells and other UBC's (Nunzi and Mugnaini, 2000; Nunzi at al., 2001). We presume similar axonal properties for mormyrid UBC's, but can not yet demonstrate it.

The proximal valvula—The proximal valvula consists of lobes C2v, C1 and LT. We will first describe the morphological specializations observed in C1, and then compare it with C2v and LT.

The most important morphological difference between lobes C1 and C3 concerns the presence of deep stellate cells in lobe C1. As described above, these are GABA-, calretinin- and calbindin-immunoreactive. The latter two antibodies reveal their morphological organization in particular detail. The cell bodies of deep stellate cells are located between the ganglionic and molecular layer (Figs. 7B, C; 8C; 9A). Their axons, which are even more strongly immunoreactive to anti-GABA, anti-calbindin and anti-calretinin than their cell bodies, have a rostrocaudal orientation and are concentrated in a distinct fiber layer between the ganglionic and granular layers (Figs. 7D; 8C; 9A). The large number of deep stellate axons within lobe C1 and C2v and their length in sagittal sections suggests that most deep stellate axons project over long rostro-caudal and/or caudo-rostral distances in these lobes. Our material shows that they innervate efferent cerebellar neurons quite densely (Fig. 9; see below).

The dendrites of deep stellate cells in lobe C1 are thin and smooth and extend into the molecular layer (Figs. 7B, D; 9A). The orientation of their dendritic tree is predominantly sagittal, although less strict than the dendritic trees of Purkinje cells and efferent cells. Deep stellate cells are smaller than Purkinje cells, i.e. on average 5 × 4 μm (the largest being 7 × 6 μm) compared with an average size of 12 × 9 μm for Purkinje cells of lobe C1 in our GABA-stained sections, and 11 × 7 μm in IP3R material. In contrast, the number of stellate cells is higher, with an average ratio of deep stellate cells versus Purkinje cells of about 2:1. This ratio was determined in GABA stains as well as by comparing Purkinje cell counts in anti-IP3R- and anti-calcineurin sections with deep stellate cell counts in comparable sections stained with anti-calretinin and anti-calbindin. Deep stellate cell bodies may have quite numerous gephyrin-immunoreactive spots on their surface (Fig. 9B), indicating that they receive a rather strong inhibitory innervation. It is presently unknown whether this originates from Purkinje cells, deep stellate cells, or both.

Efferent cells in lobe C1 are similar to those in lobe C3 in having a cell body in the deeper part of the ganglionic layer and a sagitally oriented dendritic tree with smooth dendrites in the molecular layer (Figs 7B, C). However, their apical dendrites in lobe C1 are much thicker than in lobe C3, as observed in Golgi-material (Fig.10B). They receive a similar amount of parallel-fiber synaptic contacts as Purkinje cells, however, not on spines, but directly on their smooth dendritic surface (Fig. 10C).

The somata and proximal dendrites of efferent cells in C1 are densely innervated by GAD-positive and gephyrin-immunoreactive terminals (Figs 8B; 9B-D). The density of these terminals in C1 is much greater than in the corpus. In the electron microscope, it was observed that this dense GABAergic innervation originates only minimally from Purkinje cell axons (Fig 10 D, G). By far the largest part arises from another type of axon, which is myelinated and makes terminals with a less dense cytoplasm than Purkinje cell axons (Fig. 10E, G). Our immunohistochemical data show that the dense terminal plexus around efferent cells in lobe C1 is immunoreactive to anti-calbindin and anti-calretinin (Fig 9A), which leads to the conclusion that this dense GABAergic, inhibitory innervation of the cell bodies and proximal dendrites of efferent cells in lobe C1 arises predominantly from the deep stellate cells.

The ratio of efferent cells to Purkinje cells in C1, as estimated from comparisons of gephyrin-immunoreactive sections (visualizing efferent cells) with comparable IP3R-immunoreactive sections (visualizing Purkinje cells), was about 1 : 3. This means that the ratio of efferent to deep stellate cells is about 1:6, since the ratio between Purkinje cells and deep stellate cells is about 1 : 2.

The organization of lobe C2v is similar to that of lobe C1. In fact, lobes C1 and C2v form one continuous and homogeneous, folded strip of proximal valvular tissue (Fig. 4). The organization of the transitional lobe (LT) is also similar to that of lobe C1, but with lower densities of efferent and deep stellate neurons. In addition, the granule cells of the transitional lobe are located lateral to the molecular layer, giving rise to parallel fibers without a T-shaped bifurcation (Fig. 2E). In the rostral region of LT, the molecular and ganglionic layers, but not the granular layer, bend upwards, thus establishing a gradual transition towards the ridged organization of the distal valvula (Nieuwenhuys and Nicholson, 1969a).

The distal valvula—Our immunohistochemical data show that the organization of the distal or ridged valvula is basically similar to that of the proximal valvula. The cell types and connections are similar, but they have a different topological arrangement (Fig. 11). Purkinje cells are medially located in the ridges (Fig. 11A) and are substantially smaller than in other cerebellar regions, measuring about 8 × 6 μm in both GABA- and IP3R material. This means that the volume of their cell bodies is about three times smaller than in the corpus and about 9 times smaller than in the caudal lobe. The planes of Purkinje cell dendritic trees are oriented “horizontally”, perpendicular to the parallel fibers that enter the molecular layer at the bottom of the ridges (Fig. 2F; see Shi et al., 2008).

Efferent cells are located at the base of the ridges and thus are referred to as basal cells. Most of their properties are similar to those of the efferent cells in the proximal valvula, including immunopositivity to anti-glutamate (Fig. 11E) and anti-calretinin (Fig. 11C, G), a dense GABA-, GAD- and gephyrin-positive innervation (Fig. 11F, H) and thin, smooth dendrites in the molecular layer. However, the dendritic trees of efferent cells in the distal valvula are different from those in the proximal valvula and the corpus in that they are not oriented perpendicular to the parallel fibers, and are not planar. The dendrites of basal cells extend vertically for some distance into the molecular layer in the direction of the parallel

fibers, as shown in sections stained with anti-calretinin (Fig. 11C) and anti-gephyrin (Fig. 11H) as well as in previous Golgi studies (Nieuwenhuys and Nicholson, 1969b). Calbindin-immunopositivity is found in the basal cells of a few ridges but is not present in most basal cells (see Discussion).

Deep stellate cells occur in large numbers in each valvular ridge and are located between the layer of Purkinje cells and the molecular layer (Fig. 11F). In transverse sections through ridges, we counted on average about 200 deep stellate cells, 100 Purkinje cells and 2 distinct basal cells. Similar to Purkinje cells, deep stellate cells in the ridged valvula are smaller than in C1, since they measure only about 5 × 4 μm. GABA-immunoreactivity shows that they occur throughout the basal to distal extent of the ridges (Fig. 11F). However, in material stained with anti-calbindin, only the distal 2/3 population stains (Fig. 11B). In material treated with anti-calretinin, the proximal 1/3 population, located within the confines of the dendritic tree of the basal cells, stains as well, but less intensely than the distal population, and separated from the latter by a kind of immunonegative gap (Fig. 11C). Weakly anti-CamKIIα-immunoreactive deep stellate cells occur precisely within this “gap” (Fig. 11D).

Moderately calretinin-positive axons impinge with high densities on the basal efferent cells of the ridged valvula (Fig 11C, G). However, we observed hardly any calretinin-positive axons in the distal 2/3 portion of the ridges. This strongly suggests that the dense innervation of basal cells by GABA-, GAD-, gephyrin- and calretinin-positive inhibitory terminals (Fig. 11F, H) arises predominantly or even exclusively from the deep stellate cells in the proximal 1/3 part of the ridges. The strongly calbindin- and calretinin immunopositive deep stellate cells located distally in the ridge apparently do not project to basal cells (Fig. 11B), and consequently have different axonal properties than the proximally located calbindin-negative deep stellate cells. Possibly, their axonal properties are similar to those of the “classical”, superficial stellate cells in the corpus and valvula, giving rise to the GABA-transporter 1-positive network in the molecular layer, which is also quite dense in the valvular ridges.

A final observation in the distal valvula comes from sections treated with anti-CamKIIα. In these sections, valvular ridges contained strongly immunoreactive cells resembling the “vertical” cells described by Nieuwenhuys and Nicholson (1969b; Fig. 11D). These cells are located in the Purkinje cell layer and have different properties than any of the other cells observed in our present analysis, including basal efferent cells, Purkinje cells, and deep stellate cells. Our data did not show axonal properties of these neurons, so we can not verify the suggestion by Nieuwenhuys and Nicholson (1969b) that these “vertical” cells might represent a second type of efferent neuron in the ridged valvula. However, intracellular labeling shows that they have an axon that projects outside of the slices used for labeling, with an unknown destination. Such labeling also shows that the vertical cells have several local axon collaterals (Shi et al., 2008).

DISCUSSION

Technical remarks

Our immunohistochemical study has revealed a remarkable chemical as well as morphological diversity among the different subdivisions of the mormyrid cerebellum. In

several cases, the same neuronal element was stained in some regions of the cerebellum but not in other regions. This raises the question as to whether the element is absent in a given region or is present but with a different chemical composition. The latter is clearly the case for Purkinje cell staining by Zebrin II, which is present in the corpus and most of the distal valvula but absent in the proximal valvula (Meek et al., 1992). This clearly does not mean that Purkinje cells are absent in the proximal valvula, but demonstrates instead that a subpopulation of Purkinje cells does not express Zebrin II. The same holds for the absence of staining of climbing fibers in the valvula by anti-calretinin and anti-NR1, antibodies which stain climbing fibers throughout the corpus and caudal lobe. This must also reflect a chemical differentiation, because climbing fibers are demonstrably present in the proximal and distal valvula (Kaiserman Abramof and Palay, 1969; Meek and Nieuwenhuys, 1991; Han et al., 2006; Shi et al., 2008). The same holds for cerebellar efferents. These cells are visualized in the valvula by their immunopositivity to anti-calretinin and by the high density of GABA-, GAD- and gephyrin positive terminals and synapses on their surface, but not in the corpus and caudal lobe. This does not mean that cerebellar efferent cells are absent in the corpus or caudal lobe, but only that they have different chemical and synaptic properties in these cerebellar subdivisions. Interestingly, calretinin-immunoreactivity has also been reported for subpopulations of efferent neurons and climbing fibers in the teleosts *Chelon labrosus* (Diaz-Regueira and Anadon, 2000) and *Danio rerio* (Castro et al. 2006).

In contrast, the absence of calbindin- and calretinin-immunoreactive deep stellate cells in the corpus and caudal lobe reflects the absence of these cells in the corpus and caudal lobe, as confirmed by GABA-immunohistochemistry and electron microscopy. Consequently, the presence of numerous calbindin- and calretinin-positive deep stellate cells indicates a distinct morphological specialization of the valvula. Likewise, we assume that the distribution of unipolar brush cells as found in series treated with anti-mGluR2/3, anti-calbindin and anti-calretinin shows their real morphological distribution, and that there are no unipolar brush cells that are immunonegative to these antibodies.

Immunohistochemical comparison of mormyrids and mammals

There are both clear similarities and clear differences between the immunohistochemical staining patterns in mormyrids and mammals. All Purkinje cells in both groups stain with antibodies to the IP3R1 (Takei et al., 1994), mGluR1 receptors (Gorcs et al., 1993), and calcineurin (Usuda et al., 1990). But the antibody to calbindin that we used stains mammalian (Baimbridge and Miller, 1982) but not mormyrid Purkinje cells. Purkinje cells, stellate cells, and Golgi cells all stain with antibodies to GABA in all vertebrates, including mammals, mormyrids and other fish (e.g. Castro et al. 2006, using zebrafish). However, Golgi cells in the mammal stain with antibodies to mGluR2/3 receptors (Ohishi et al. 1994) but did not do so in the mormyrid. Some but not all climbing fibers stain with an antibody to calretinin in mammals (Yan and Garey 1998), mormyrids and other teleosts (Diaz-Regueira and Anadon, 2000; Castro et al., 2006). UBC's stain with antibodies to calbindin, calretinin, and mGluR2/3 in both mormyrids and mammals (Dino et al. 1994; Floris et al. 1994; Jaarsma et al. 1995).

Comparison of mormyrid and mammalian cerebellar circuitry

There are five notable differences in cerebellar organization in mormyrids compared with mammals, as outlined in the introduction (Fig. 12A, B): 1) efferent cells are located in the ganglionic layer between the Purkinje cells and not in deep cerebellar nuclei; 2) an important population of mossy fibers originates from a large and well differentiated nucleus lateralis valvulae in the midbrain, which is absent in mammals; 3) cerebellar climbing fiber input is restricted to the soma and proximal dendrites of Purkinje cells; 4) basket cells are absent; and 5) the spiny dendrites of Purkinje cells have a palisade pattern. Mormyrids share the first four differences with other teleosts, whereas the palisade pattern is a mormyrid specialization, not observed in any other vertebrate group.

The location of efferent cells in the ganglionic layer and the presence of a precerebellar nucleus lateralis valvulae are teleostean specialization, shared with at least one other actinopterygian group, the chondrosteans (Huesa at al., 2003). It is derived from the basic vertebrate pattern encountered in other vertebrate groups with a clear cerebellum, including cartilaginous fishes (Alvarez-Otero et al. 1996; Smeets, 1997), amphibians, reptiles, birds and mammals (Nieuwenhuys et al., 1997). In the basic vertebrate pattern, efferent cerebellar cells are concentrated in deep cerebellar nuclei and a precerebellar nucleus lateralis valvulae is absent. In contrast, the absence of climbing fiber projections throughout the molecular layer and the absence of basket cells in mormyrids may be considered as a plesiomorphic or “primitive”, basic vertebrate condition, from which the more derived mammalian organization, with climbing fibers that climb throughout the molecular layer and with basket cells, has evolved. As discussed by Meek and Nieuwenhuys (1991) and Meek (1992a), the mammalian configuration can be considered as a climbing fiber specialization, extending and optimizing the effect of climbing fibers, whereas the mormyrid configuration with its palisade pattern can be considered as a parallel fiber specialization, optimizing the processing of parallel fiber input.

The most crucial difference between the cerebellum of actinopterygians, including mormyrids, and the cerebella of other vertebrate groups is the location of efferent cells within the cerebellar cortex. All other vertebrate groups with distinct cerebella have deep cerebellar nuclei giving rise to cerebellar efferent projections (Nieuwenhuys et al., 1997). Most likely, efferent teleostean cerebellar cells can be considered as migrated deep cerebellar nuclear cells, but this has not been determined with certainty by experimental embryological techniques.

The location of efferent cells in the ganglionic layer, with dendrites in the molecular layer, means that their excitatory input comes from parallel fibers, instead of mossy fibers as occurs with mammalian deep nucleus neurons. Consequently, their excitatory input is much more similar, in space, in time, and in information conveyed, to that of Purkinje cells than is the case for mammalian deep cerebellar nucleus cells and mammalian Purkinje cells. The parallel fiber input of efferent cells is almost identical to that of neighboring Purkinje cells. However, efferent cell dendrites have no spines, which suggests that their parallel fiber synapses are less plastic than those of Purkinje cells, or not plastic at all. Moreover, efferent cells do not receive olivocerebellar (“climbing fiber”) input, in contrast to mammalian deep

cerebellar neurons, which do receive input from olivocerebellar collaterals (Ito, 1984; Shinoda et al., 2000)

Efferent cells in the corpus receive a moderate number of inhibitory Purkinje axonal synaptic contacts on their somatic and proximal dendritic surface (compare Meek and Nieuwenhuys, 1991 with fig. 10F). Compared with the huge parallel fiber input to efferent cells, the number of Purkinje axonal terminals on efferent cells is surprisingly low. It is clear that Purkinje cells are numerous and very regularly organized in the mormyrid cerebellum, and thus seem to be important elements, if not the most important elements. However, they can only influence cerebellar targets via efferent cells, which receive only a surprisingly small amount of Purkinje axon terminals. It is clear that more physiological studies are necessary to analyze this apparent paradox of massive distal parallel fiber input contrasting with minimal proximal Purkinje cell input and to investigate the functional roles and interrelations of Purkinje cells and efferent cells. In addition to Purkinje axonal input, the cell bodies and proximal dendrites of efferent cells in the mormyrid corpus receive another type of inhibitory input (Fig. 10F). Comparison with the valvula strongly suggests that this input arises from stellate cells (see below).

The restriction of climbing fiber input to the ganglionic layer of mormyrids and other teleosts means that many parallel fiber inputs are at a considerable distance from the climbing fiber input, in contrast to mammalian Purkinje cells, where spiny branchlets are short and climbing fiber synapses are closer on average to parallel fiber synapses. The functional consequences of the greater distance between the two inputs in mormyrids will depend in part on the postsynaptic responses of Purkinje cells. For example, dendritic spikes may be generated by climbing fiber input at the base of the cell and propagated out into the long, spiny palisade dendrites, allowing for plastic or other types of interactions between climbing fiber and parallel fiber inputs. Broad spikes that are different from axon spikes are indeed recorded from mormyrid Purkinje cells in the central lobes and these spikes are sometimes evoked by climbing fiber activation (Han and Bell, 2003), but it is not yet known if these spikes propagate out into the palisade dendrites.

Nevertheless, the anatomy suggests that the effect of climbing fiber input on parallel fiber synapses may be less direct, less stereotyped and more malleable in mormyrid than in mammalian Purkinje cells. Dendritic spikes in the long palisade dendrites may, for example, be susceptible to modification by inhibitory or excitatory inputs. Thus, cerebellar learning, mediated by climbing fiber induced plasticity of parallel fiber input (Ito, 1984) may be less precisely and tightly controlled by the inferior olive in mormyrids than in mammals. The long spiny dendrites covered with parallel fiber synapses and without climbing fiber contacts also suggests a greater degree of interactions among different parallel fiber inputs, including forms of associative plasticity that do not require the climbing fiber.

Basket cells are found only in mammals and birds. They receive parallel fiber input and densely innervate the somata and initial segments of Purkinje cells with basket-shaped terminal arbors, thus exerting a strong inhibitory effect on Purkinje cells (Fig. 12A, B; Ito, 1984; Nieuwenhuys et al., 1997). Basket cells therefore reduce the excitatory effect of parallel fibers relative to that of climbing fibers. Thus the presence of basket cells in

mammals but not teleosts and the difference in spatial separation of parallel and climbing fiber inputs in the two groups support the conclusion of Meek and Nieuwenhuys (1991) that the mammalian cerebellum is a climbing fiber specialization, whereas the teleostean cerebellum, and especially the mormyrid cerebellum with its palisade pattern, is a parallel fiber specialization.

Functional implications of mormyrid cerebellar specializations

In addition to the differences between mammals and mormyrids discussed in the preceding paragraph, the present study has demonstrated or confirmed a number of mormyrid specializations that are not shared with other teleosts, including: 1) the palisade pattern of Purkinje cell dendrites in the corpus and valvula; 2) the near random distribution of Purkinje cell dendrites and minimal sagittal organization in the caudal lobe; and 3) the presence of deep stellate cells and several topological transformations in the valvula.

The palisade pattern—The orthogonal relation between parallel fibers and Purkinje cell dendrites in most cerebellar structures has been considered to be a mechanism for detecting coincidences among parallel fibers (Braitenberg, 1967; Braitenberg et al., 1997; Meek, 1992b). The unusual palisade pattern of mormyrids extends the orthogonal organization of the molecular layer into the third dimension, and suggests that some particular spatial patterns of parallel fiber activity might be especially effective in driving mormyrid Purkinje cells. Specific hypotheses as to which patterns might be most effective will require a clearer understanding of postsynaptic processing and spike generating mechanisms in mormyrid Purkinje cells. If, for example, dendritic spikes are readily evoked within a single palisade dendrite, and if such dendritic spikes can propagate to the soma to trigger a Purkinje cell spike, then a vertically oriented strip of synchronized parallel fiber activity might be especially effective. But if such dendritic spikes are not prominent, then a horizontally oriented strip of synchronized parallel fiber activity might result in summation of the EPSPs from the different dendrites at the base of the cell and so be a more effective pattern of parallel fiber input.

The caudal cerebellar lobe—Purkinje cells in most parts of the caudal lobe do not have a palisade pattern and most cells do not even have a strictly sagittal orientation of their dendritic trees (Campbell et al., 2007). This relative lack of organization in comparison to the corpus and valvula suggests a poor capacity for detecting spatio-temporal input patterns by coincidence detection and in relaying the results of such detection in a well ordered manner by a set of Purkinje cells. In addition, the present study shows that UBC’s are especially prominent in the granular eminences that provide parallel fibers to the caudal lobe. In mammals, it has been shown that UBC’s receive mossy fiber input and generate long bursts of spikes upon activation, which are conveyed via short axons to nearby granule cells and other UBC’s (Rossi et al., 1995; Nunzi and Mugnaini, 2000; Nunzi et al., 2001). The UBC’s therefore amplify mossy fiber input both in time and space, and reduce specific spatio-temporal mossy fiber input patterns. Thus, the organization of the caudal lobe and the granular eminences may not be suited for discrimination of spatio-temporal patterns like the corpus, but may instead be involved in amplifying and distributing mossy fiber activity.

Interestingly, the processing of mossy fiber input signals in the posterior caudal lobe is working in parallel with the processing of similar mossy fiber input in the electrosensory lateral line lobe (ELL), located underneath the posterior caudal lobe (Fig. 3a,b). Both structures receive parallel fiber input from the eminentia granularis posterior (EGp) and project to the same midbrain structures, i.e. the preeminential nucleus and the lateral toral nucleus (Bell et al., 1981; Meek et al., 1999; Campbell et al., 2007). It has been suggested that the electrosensory input to the deeper layers of the cerebellum-like ELL is similar in some respects to the climbing fiber input to the cerebellum. In both cases, an association of these inputs with parallel fiber input appears to result in plastic changes at the parallel fiber synapse in such a way that parallel fiber activity comes to predict electrosensory input in the case of ELL and climbing fiber input in the case of the cerebellum. (Bell et al., 1997; Bell, 2002; Bell et al., 2008). Thus, the ELL and the posterior caudal lobe appear to process similar parallel fiber input and mediate adaptive learning that is “supervised” in ELL by primary afferent input and in the posterior caudal lobe by olivocerebellar input. The results from both structures are subsequently integrated in the midbrain. Unfortunately, the functional and behavioral significance of the olivocerebellar climbing fiber input to the caudal lobe is presently unclear.

The proximal valvula—The valvula shows a number of additional specializations in comparison to the corpus. These include: an even more regular palisade pattern with less branching points in the molecular layer compared with the corpus (Meek and Nieuwenhuys, 1991; Han et al., 2006), several topological transformations resulting in different patterns of parallel fiber projections to the molecular layer (Nieuwenhuys and Nicholson, 1969a; Meek, 1992b); and the presence of a “new” cell type, the deep stellate cell.

Deep stellate cells resemble basket cells in being GABAergic and in having sagittally projecting axons. However, they terminate massively on efferent cells instead of on Purkinje cells (Figs. 12 A, C). The sagittal projection of deep stellate cell axons suggests they inhibit efferent cells located more rostrally and caudally, but not laterally. Purkinje cell axons also project sagittally over considerable rostro-caudal distances (Han et al., 2006). So, both inhibitory axonal projections in the ganglionic layer of the proximal valvula seem to inhibit efferent cells exclusively in the sagittal direction. We observed that the axons of deep stellate cells are myelinated, (in contrast to those of Purkinje cells, see Meek and Nieuwenhuys, 1991) which suggests that the inhibitory effects of deep stellate cells are faster and extend further than those of Purkinje cells. The widespread sagittal projections of both Purkinje cells and deep stellate cells suggest that both inhibitory systems enhance a focus of mossy fiber activity in the rostrocaudal direction by inhibiting the effects of mossy fiber inputs that arrive later in more rostral or caudal regions.

The huge inhibitory input of deep stellate cells onto efferent cells in the proximal valvula raises a major question as to the role of Purkinje cells in this part of the cerebellum. As discussed above, in the corpus, efferent cells are inhibited by Purkinje cells. Although the number of Purkinje axonal synapses on efferent cells in the corpus is relatively low, their proximal position might still allow for substantial inhibition of efferent cells in the same way as that mammalian Purkinje cells inhibit deep cerebellar nucleus neurons. In the valvula, however, the inhibitory effect of Purkinje cells on efferent cells seems to be minimal in

comparison to the inhibitory effect of deep stellate cells. In the proximal valvula (lobe C1), the ratio of deep stellate axon terminals versus Purkinje axonal terminals on efferent cells is about 15:1 (Fig. 10G). In the ridged valvula, direct Purkinje cell input onto efferent cells might even be absent (see below).

Efferent cells, deep stellate cells and Purkinje cells all receive similar and simultaneous parallel fiber input in any local region of the proximal valvula (Fig. 12C). A parallel fiber pattern that is large enough and simultaneous enough, might result in spike generation by efferent cells, but this will be followed very soon by inhibition from activated deep stellate cells. The high density of stellate axon terminals on efferent cells suggests that the resulting inhibition is very strong and long lasting. So, the question arises as to what might be added to this strong deep stellate cell inhibition by the weaker and possibly later Purkinje cell inhibition. Purkinje cells are numerous, highly organized and the major, if not the only, target of climbing fiber input, but their function in the proximal valvula is uncertain. The termination pattern of Purkinje cells in the proximal valvula is not yet well described, and one possibility is that Purkinje cell axons terminate on and inhibit deep stellate cells. That would lead to the rather remarkable consequence that Purkinje cells have a predominantly disinhibitory effect on efferent cells. Electrophysiological recordings with morphological identification, possibly involving two cell recording, will be required to establish the role of Purkinje cells in the valvula.

The ridged valvula—The histological organization of the ridged valvula, with its basal efferent cells, deep stellate cells and Purkinje cells, is even more puzzling than the organization of the proximal valvula (Fig. 12D). Intriguing features in this largest part of the mormyrid cerebellum include the following: 1) parallel fibers enter the molecular layer of the ridges from only one side and so lack the usual T junction and ascending branch; 2) the dendritic trees of basal efferent cells are neither planar nor sagittally (or, in the coordinates of the valvular ridges, horizontally) oriented, 3) the proximal, but not the distal deep stellate cells project to the basal efferent cells; and 4) most Purkinje cells do not seem to project at all to basal efferent cells, since their axons are sagitally oriented, parallel to the dendritic trees of the Purkinje cells (Shi et al., 2008). The latter implies that Purkinje cell axons probably terminate exclusively on the deep stellate cells and/or on other Purkinje cells. This would mean that the circuitry of the proximal one third of the ridges is similar to the circuitry described above for the proximal valvula (Fig 12C, D).

The role of the distal two thirds of the ridge is especially puzzling. The Purkinje cells as well as the deep stellate cells in this region do not project to basal efferent cells, so it is unclear how they might influence cerebellar output. Most likely, there is another type of efferent cell in the distal part of the ridges that is different from the basal cell. One candidate is the “vertical cell”, visualized in the present study with anti-CamK2α, which is similar to the vertical cell described by Nieuwenhuys and Nicholson (1969b) on the basis of Golgi impregnation, and which they suggested to be an efferent cell. However, these cells have not been labeled convincingly and in large numbers in retrograde tracer studies that do show labeling of many basal efferent cells (personal observations). Moreover, these vertical cells are not densely covered with GAD- and gephyrin positive spots, which would be expected

for efferent cells of the distal ridges that receive extensive input from axon terminals of deep stellate cells or Purkinje cells.

In conclusion, we have described a new cell type, the deep stellate cell, that is present in large numbers throughout the valvula. We have also given some indication of their synaptic relations and some suggestions as to their functional role in the proximal valvula as well as in the proximal part of the ridges of the distal valvula. Their connectivity and role in the distal part of the ridges remains to be elucidated.

Acknowledgments

Grant sponsor: NIH/NINDS NS44961 to V.H. and NIH MH49792 and MH60996 to C.B.

Dedicated to Rudolf Nieuwenhuys, on the occasion of his 80th Birthday, June 11, 2007

ABBREVIATIONS

a	anterior
ax	axon
B	basal cell
bolf	bulbus olfactorius (= olfactory bulb)
c	caudal
calret	calretinin
CamKIIα	Calcium calmodulin kinase subunit IIα
Cereb	cerebellum
clf	climbing fiber
Co	corpus cerebelli
cr.cereb	crista cerebellaris (=cerebellar crest)
C1	first cerebellar lobe
C2	second cerebellar lobe
C3	third cerebellar lobe
C4	fourth cerebelar lobe
d	dorsal
di	distal
dst	deep stellate cell
E	efferent cerebellar cell (= eurydendroid cell)

EG	eminentia granularis (= granular eminence)
ELL	electrosensory lateral line lobe
G	Golgi cell
GABA	γ-aminobutyric acid
GAD	glutamic acid decarboxilase
GluR1α	Glutamate receptor subunit 1α
ggl	ganglionic layer (= layer of Purkinje cells and efferent cells)
gr(an)	granular layer
grc	granule cell
IP3R	inositol triphosphate receptor
l	lateral
LC	lobus caudalis (= caudal lobe)
lobll	lobus lineae lateralis (= ELL)
lob trans	trans lobus transitorius (=LT)
LT	lobus transitorius (= transitional lobe)
LTD	long term depression
m	myelin
mf	mossy fiber
mGluR2/3	metabotropic glutamate receptor subunit 2/3
mes(enc)	mesencephalon
mol	molecular layer
MON	medial octavolateral nucleus
NMDA	N-methyl-D-aspartate
NR1	NMDA receptor subunit 1
nlv	nucleus lateralis valvulae
p	posterior
P	Purkinje Cell
pf	parallel fiber
pr	proximal

rhombenc	rhombencephalon
sst	superficial stellate cell
st	stellate cell
tect	tectum mesencephali (= midbrain tectum)
telenc	telencephalon
UBC	unipolar brush cell
V	valvula
v	ventral
Ve	vertical cell (in Vr)
Vp	proximal valvula
Vr(idg)	ridged valvula

LITERATURE CITED

Alvarez-Otero R, Pérez SE, Rodríguez MA, Adrio F, Anadón R. GABAergic neuronal circuits in the cerebellum of the dogfish *Scyliorhinus canicula* (Elasmobranchs): an immunocytochemical study. Neurosc Lett. 1995; 187:87–90.

Alvarez-Otero R, Pérez SE, Rodríguez MA, Anadón R. Organisation of the cerebellar nucleus of the Dogfish, *Scyliorhinus canicula* L.: A light microscopic, immunocytochemical and ultrastructural study. J Comp Neurol. 1996; 368:487–502. [PubMed: 8744438]

Baimbridge KG, Miller JJ. Immunohistochemical localization of calcium-binding protein in the cerebellum, hippocampal formation and olfactory bulb of the rat. Brain Res. 1982; 245:223–229. [PubMed: 6751467]

Bell, CC. Electroreception in mormyrid fish: central physiology. In: Bullock, TH., Heiligenberg, W., editors. Electroreception. John Wiley & Sons, Inc.; New York: 1986. p. 423-452.

Bell CC. Evolution of cerebellum-like structures. Brain Behav Evol. 2002; 59:312–326. [PubMed: 12207086]

Bell, CC., Szabo, T. Electroreception in mormyrid fish: central anatomy. In: Bullock, TH., Heiligenberg, W., editors. Electroreception. John Wiley & Sons, Inc.; New York: 1986. p. 375-421.

Bell CC, Bodznick D, Montgomery J, Bastian J. The generation and substraction of sensory expectations within cerebellum-like structures. Brain Behav Evol. 1997; 50:17–31. [PubMed: 9217991]

Bell CC, Finger TE, Russell CJ. Central connections of the posterior lateral line lobe in mormyrid fish. Exp Brian Res. 1981; 42:9–22.

Bell CC, Han V, Sawtell NB. Cerebellum-like structures and their implications for cerebellar function. Ann Rev Neurosci. 2008 in press.

Bell CC, Han VZ, Sugawara Y, Grant K. Synaptic plasticity in the mormyrid electrosensory lobe. J Exp Biol. 1999; 202:1339–1347. [PubMed: 10210674]

Bell CC, Meek J, Yang JY. Immunocytochemical identification of cell types in the mormyrid electrosensory lobe. J Comp Neurol. 2005; 483:124–142. [PubMed: 15672392]

Bottai D, Dunn RJ, Ellis W, Maler L. N-methyl-D-aspartate receptor 1 mRNA distribution in the central nervous system of the weackly electric fish *Apteronotus leptorhynchus*. J Comp Neurol. 1997; 389:65–80. [PubMed: 9390760]

Braitenberg V. Fox A, Snider RS. Is the cerebellar cortex a biological clock in the millisecond range? The Cerebellum. Progress Brain Res. 1967; 25:334–346.

Braitenberg V, Heck D, Sultan F. The detection and generation of sequences as a key to cerebellar function: experiments and theory. Behav Brain Sci. 1997; 20(2):229–45. [PubMed: 10096998]

Brochu G, Maler L, Hawkes R. Zebrin II: a polypeptide antigen expressed selectively by Purkinje cells reveals compartments in rat and fish cerebellum. J Comp Neurol. 1990; 291:538–52. [PubMed: 2329190]

Bueno OF, Wilkins BJ, Tymitz KM, Glascock BJ, Kimball TF, Lorenz JN, Molkentin JD. Impaired cardiac hypertrophic response in Calcineurin Abeta -deficient mice. Proc Natl Acad Sci. 2002; 99:4586–91. [PubMed: 11904392]

Campbell HR, Meek J, Zhang J, Bell CC. Anatomy of the posterior caudal lobe of the cerebellum and the eminentia granularis posterior in a mormyrid fish. J Comp Neurol. 2007; 502:714–735. [PubMed: 17436286]

Carr, CE., Maler, L. Electroreception in Gymnotiform fish. Central anatomy and physiology. In: Bullock, TH., Heiligenberg, W., editors. Electroreception. John Wiley & Sons, Inc.; New York: 1986. p. 319-373.

Castro A, Becerra M, Manso MJ, Anadón R. Calretinin immunoreactivity in the brain of the zebrafish, *Danio rerio*: Distribution and comparison with some neuropeptides and neurotransmitter-synthesizing enzymes. II. Midbrain, hindbrain and rostral spinal cord. J Comp Neurol. 2006; 494:792–814. [PubMed: 16374815]

Díaz-Regueira S, Anadón R. Calretinin expression in specific neuronal systems in the brain of an advanced teleost, the Grey Mullet (*Chelon labrosus*). J Comp Neurol. 2000; 426:81–105. [PubMed: 10980485]

Dino MR, Willard FH, Mugnaini E. Distribution of unipolar brush cells and other calretinin immunoreactive components in the mammalian cerebellar cortex. J Neurocytol. 1999; 28:99–123. [PubMed: 10590511]

Erondu NE, Kennedy MB. Regional Distribution of type II Ca^{2+} / calmodulin-dependent protein kinase in rat brain. J Neurosci. 1985; 5:3270–3277. [PubMed: 4078628]

Finger TE. Efferent neurons of the teleost cerebellum. Brain Res. 1978; 153:608–614. [PubMed: 81089]

Finger, TE. The organization of the cerebellum in teleosts. In: Northcutt, RG., Davis, RE., editors. Fish neurobiology and behavior. University of Michigan Press; Ann Arbor, MI: 1983. p. 261-284.

Finger TE, Bell CC, Russell CJ. Electrosensory pathways to the valvula cerebelli in mormyrid fish. Exp Brain Res. 1981; 42:23–33. [PubMed: 6163654]

Floris A, Dino M, Jacobowitz DM, Mugnaini E. The unipolar brush cells of the rat cerebellar cortex and cochlear nucleus are calretinin-positive: a study by light and electron microscopic immunocytochemistry. Anat Embryol (Berl). 1994; 189:495–520. [PubMed: 7978355]

Gorcs TJ, Penke B, Boti Z, Katarova Z, Hamori J. Immunohistochemical visualization of a metabotropic glutamate receptor. Neuroreport. 1993; 4:283–6. [PubMed: 7682854]

Han VZ, Bell CC. Physiology of cells in the central lobes of the mormyrid cerebellum. J Neurosci. 2003; 23:11147–11157. [PubMed: 14657174]

Han VZ, Meek J, Campbell HR, Bell CC. Cell morphology and circuitry in the central lobes of the mormyrid cerebellum. J Comp Neurol. 2006; 497:309–325. [PubMed: 16736465]

Han VZ, Zhang Y, Bell CC, Hansel C. Synaptic plasticity and calcium signalling in Purkinje cells of the central cerebellar lobes of mormyrid fish. J Neurosci. 2007; 27:13499–512. [PubMed: 18057208]

Huesa G, Anadón R, Yáñez J. Afferent and efferent connections of the cerebellum of the chondrostean *Acipenser baeri*: A carbocyani9ni dye (DiI) tracing study. J Comp Neurol. 2003; 460:327–344. [PubMed: 12692853]

Ito, M. The cerebellum and neural control. Raven Press; New York: 1984.

Ito H, Yoshimoto M. Cytoarchitercure and fiber connections of the nucleus lateralis valvulae in the carp (*Cyprinus carpio*). J Comp Neurol. 1990; 298:385–399. [PubMed: 2229471]

Jaarsma D, Dino MR, Ohishi H, Shigemoto R, Mugnaini E. Metabotropic glutamate receptors are associated with non-synaptic appendages of unipolar brush cells in rat cerebellar cortex and cochlear nuclear complex. J Neurocytol. 1998; 27:303–27. [PubMed: 9923978]

Kaiserman-Abramof, IR., Palay, SL. Fine structural studies of the cerebellar cortex in a mormyrid fish. In: Llinás, RR., editor. Neurobiology of cerebellar evolution and development. Am Med Ass Educ & Res Found.; Chicago: 1969. p. 171-205.

Kaufman DL, Houser CR, Tobin AJ. Two forms of the y-aminobutyric acid synthetic enzyme glutamate decarboxylase have distinct intraneuronal distributions and cofactor interactions. Neurochem. 1991; 56:720–723.

Larsell, O. The comparative anatomy and histology of the cerebellum from myxinoids through birds. Jansen, J., editor. University of Minneapolis Press; Minneapolis: 1967.

Meek J. Comparative aspects of cerebellar organization. From mormyrids to mammals. Eur J Morphol. 1992a; 30:37–51. [PubMed: 1642952]

Meek J. Why run parallel fibers parallel. Teleostean Purkinje cells as possible coincidence detectors, in a timing device subserving spatial coding of temporal differences. Neuroscience. 1992b; 48:249–283. [PubMed: 1603322]

Meek J. The cerebellum and timing: Lessons from mormyrids. Behav. Brain Sci. 1997; 20:258.

Meek J, Nieuwenhuys R. Palisade pattern of mormyrid Purkinje cells: a correlated light and electron microscopic study. J Comp Neurol. 1991; 306:156–192. [PubMed: 2040726]

Meek, J., Nieuwenhuys, R. Holosteans and teleosts. In: Nieuwenhuys, R.Ten Donkelaar, HJ., Nicholson, C., editors. The central nervous system of vertebrates. Vol. 2. Springer Verlag; Berlin: 1997. p. 759-938.

Meek J, Hafmans TGM, Maler L, Hawkes R. Distribution of zebrin II in the gigantocerebellum of the mormyrid fish *Gnathonemus petersii* compared with other teleosts. J Comp Neurol. 1992; 316:17–31. [PubMed: 1573049]

Meek J, Nieuwenhuys R, Elsevier D. Afferent and efferent connections of cerebellar lobe C1 of the mormyrid fish *Gnathonemus petersii*: an HRP study. J Comp Neurol. 1986a; 245:319–341. [PubMed: 3958249]

Meek J, Nieuwenhuys R, Elsevier D. Afferent and efferent connections of cerebellar lobe C3 of the mormyrid fish *Gnathonemus petersii*: an HRP study. J Comp Neurol. 1986b; 245:342–358. [PubMed: 2870092]

Meek J, Grant K, Bell C. Structural organization of the mormyrid electrosensory lateral line lobe. J Exp Biol. 1999; 202:1291–1300. [PubMed: 10210669]

Meek J, Hafmans TGM, Han V, Bell CC, Grant K. Myelinated dendrites in the mormyrid electrosensory lobe. J Comp Neurol. 2001; 431:255–275. [PubMed: 11170004]

Meek J, Kirchberg G, Grant K, von der Emde G. Dye coupling without gap junctions suggests excitatory connections of γ-aminobutyric acidergic neurons. J Comp Neurol. 2004; 468:151–164. [PubMed: 14648676]

Mignery GA, Sudhof TC, Takei K, De Camilli P. Putative receptor for inositol 1,4,5-triphosphate similar to ryanodine receptor. Nature. 1989; 342:192–195. [PubMed: 2554146]

Minelli A, Brecha NC, Karschin C, DeBiasi S, Conti F. GAT-1, a high-affinity GABA plasma membrane transporter, is localized to neurons and astroglia in the cerebral cortex. J Neurosci. 1995; 15:7734–46. 1995. [PubMed: 7472524]

Murakami T, Morita Y. Morphology and distribution of the projection neurons in the cerebellum in a teleost: *Sebastiscus marmoratus*. J Comp Neurol. 1987; 256:607–623. [PubMed: 3558892]

Nieuwenhuys R. Fox CA, Snider RS. Comparative anatomy of the cerebellum. The Cerebellum. Progress Brain Res. 1967; 25:1–93.

Nieuwenhuys R, Nicholson C. The cerebellum of mormyrids. Nature. 1967; 215:764–765. [PubMed: 4168449]

Nieuwenhuys, R., Nicholson, C. A survey of the general morphology, the fiber connections, and the possible functional significance of the gigantocerebellum of mormyrid fishes. In: Llinás, RR., editor. Neurobiology of cerebellar evolution and development. Am Med Ass Educ & Res Found.; Chicago: 1969a. p. 107-134.

Nieuwehuys, R., Nicholson, C. Aspects of the histology of the crebellum of mormyrid fishes. In: Llinás, RR., editor. Neurobiology of cerebellar evolution and development. Am Med Ass Educ & Res Found.; Chicago: 1969b. p. 135-169.

Nieuwenhuys R, Pouwels E, Smulders-Kersten E. The neuronal organization of cerebellar lobe C1 in the mormyrid fish *Gnathonemus petersii* (teleostei). Z Anat Entwickl-Gesch. 1974; 144:315–336.

Nieuwenhuys, R.Ten Donkelaar, HJ., Nicholson, C., editors. The central nervous system of vertebrates. Springer Verlag; Berlin: 1997.

Nilsson GE. Brain and body oxygen requirements of *Gnathonemus petersii*, a fish with an exceptionally large brain. J Exp Biol. 1996; 199:603–609. [PubMed: 9318319]

Nunzi MG, Mugnaini E. Unipolar brush cell axons form a large system of intrinsic mossy fibers in the postnatal vestibulocerebellum. J Comp Neurol. 2000; 422:55–65. [PubMed: 10842218]

Nunzi MG, Birnstiel S, Bhattacharyya BJ, Slater NT, Mugnaini E. Unipolar brush cells form a glutamatergic projection system within the mouse cerebellar cortex. J Comp Neurol. 2001; 434:329–341. [PubMed: 11331532]

Ohishi H, Ogawa-Meguro R, Shigemoto R, Kaneko T, Nakanishi S, Mizuno N. Immunohistochemical localization of metabotropic glutamate receptors, mGluR2 and mGluR3, in rat cerebellar cortex. Neuron. 1994; 13:55–66. [PubMed: 8043281]

Pfeiffer F, Simler R, Grenningloh G, Betz H. Monoclonal antibodies and peptide mapping reveal structural similarities between the subunits of the glycine receptor of rat spinal cord. Proceedings of the National Academy of Sciences USA. 1984; 81:7224–7.

Pouwels E. On the development of the cerebellum of the trout, *Salmo gairdneri*. IV. Development of the pattern of connectivity. Anat Embryol. 1978; 153:55–56. [PubMed: 655438]

Ramón y Cajal, S. Histologie du système nerveux de l'homme et des vertébrés I et II. Maloine; Paris: 1911.

Rogers JH. Immunoreactivity for calretinin and other calcium-binding proteins in cerebellum. Neuroscience. 1989; 31:711–721. [PubMed: 2594199]

Rossi DJ, Alford S, Mugnaini E, Slater NT. Properties of transmission at a giant glutamatergic synapse in cerebellum: the mossy fiber-unipolar brush cell synapse. J Neurophysiol. 1995; 74:24–42. [PubMed: 7472327]

Shi Z, Zhang Y, Meek J, Qiao J, Han VZ. The unusual neuronal organization of a remarkable cerebellar specialization: the valvula cerebelli of a mormyrid fish. J Comp Neurol. 2008 in press.

Shinoda Y, Sugihara I, Wu HS, Sugiuchi Y. The entire trajectory of single climbing and mossy fibers in the cerebellar nuclei and cortex. Prog Brain Res. 2000; 124:173–86. [PubMed: 10943124]

Stendell W. Die Faseranatomie des Mormyriden Gehirns. Abh Senckenb Naturforsch Gesch. 1914; 36:3–40.

Takei K, Mignery GA, Mugnaini E, Sudhof TC, De Camilli P. Inositol 1,4,5-trisphosphate receptor causes formation of ER cisternal stacks in transfected fibroblasts and in cerebellar Purkinje cells. Neuron. 1994; 12:327–42. [PubMed: 8110462]

Usuda N, Arai H, Sasaki H, Hanai T, Nagata T, Muramatsu T, Kincaid RL, Higuchi S. Differential cellular localization of neural isoforms of the catalytic subunit of calmodulin-dependent protein phosphatase (calcineurin) in central nervous system neurons: immunohistochemistry on formalin-fixed paraffin sections employing antigen retrieval by microwave irradiation. J Histochem Cytochem. 1996; 44:13–8. [PubMed: 8543776]

Yan XX, Garey LJ. Complementary distributions of calbindin, parvalbumin and calretinin in the cerebellar vermis of the adult cat. J Hirnforsch. 1998; 39:9–14. [PubMed: 9672106]

Zhang J, Han VZ, Meek J, Bell CC. Granular cells of the mormyrid electrosensory lobe and postsynaptic control over presynaptic spike occurrence and amplitude through an electrical synapse. J Neurophysiol. 2007; 97:2191–2203. [PubMed: 17229820]

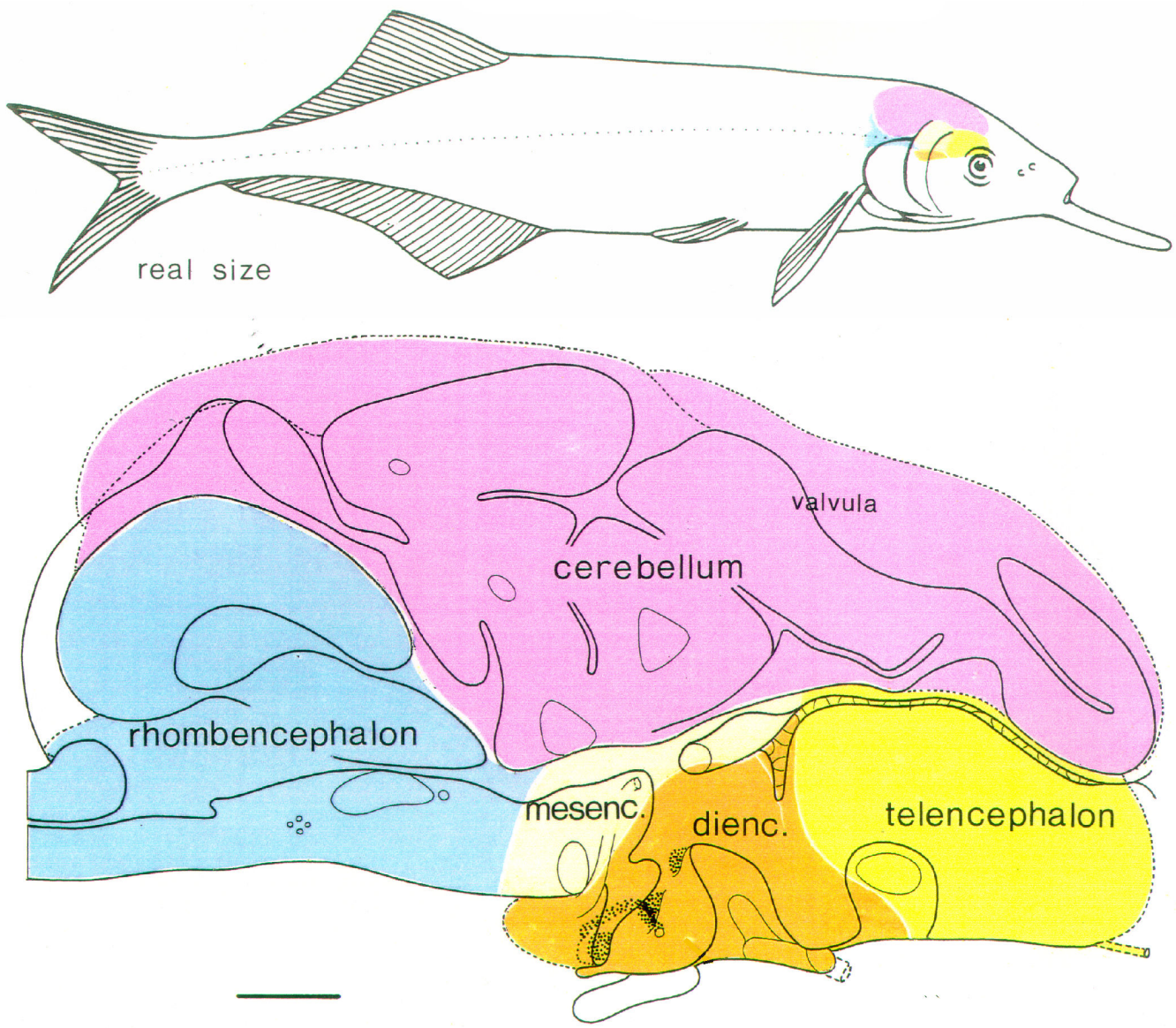

Fig. 1.

The brain of the mormyrid fish *Gnathonemus petersii*. Upper part: a lateral view of the brain in situ, illustrating the relatively large size of the cerebellum. Lower part: schematic drawing of a midsagittal section showing the location of the cerebellum on top of all other subdivisions of the brain. In this figure, the telencephalon is yellow; the diencephalon is brown; the mesencephalon is grey; the rhombencephalon is blue and the cerebellum is purple. Scale bar = 1 mm in lower panel.

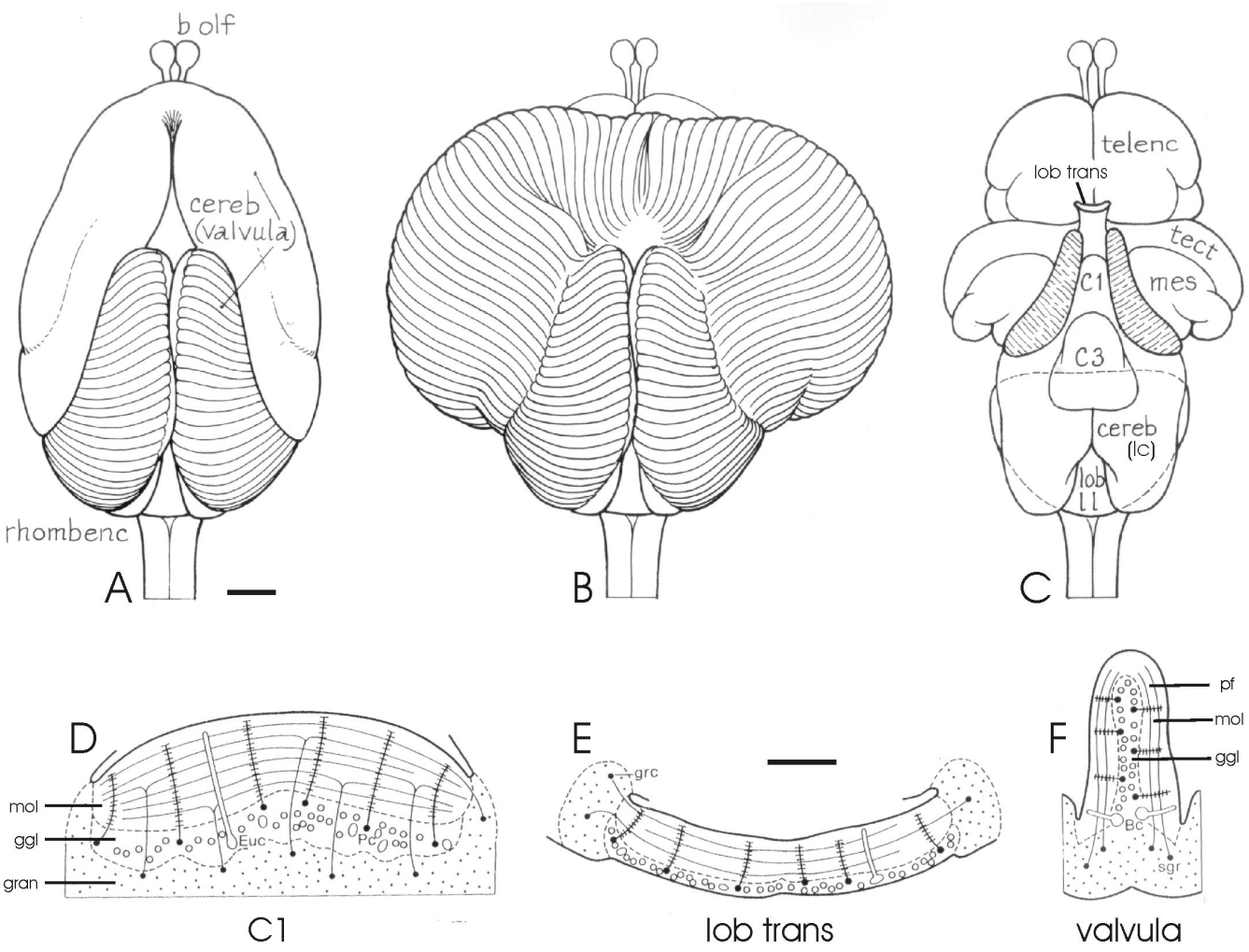

Fig. 2.

The valvula cerebelli of *Gnathonemus petersii*. A-C: Drawings of dorsal views of the brain. **A:** The valvula in its normal, intact position. **B:** The valvula unfolded to show the originally dorsal position of all valvular ridges. **C:** The valvula removed, to show the underlying brain structures. D-F: Schematic drawings of transverse sections through the valvula at the different levels. **D:** Lobe C1. **E:** The lobus transitorius. **F:** A valvular ridge. Notice the different location of the molecular and ganglionic layer with respect to the granular layer in D-F. Adapted with permission from Nieuwenhuys and Nicholson, 1969a (A-C) and Meek and Nieuwenhuys, 1997 (D-F). Abbreviations are explained in the list of abbreviations except for: Bc: basal cell (=B); Euc: eurydendroid cell (= E); Pc: Purkinje cell (=P); sgr: stratum granulare (= gran). Scale bar = 1 mm in A (applies to A-C); 100 μm in E (applies to E-G).

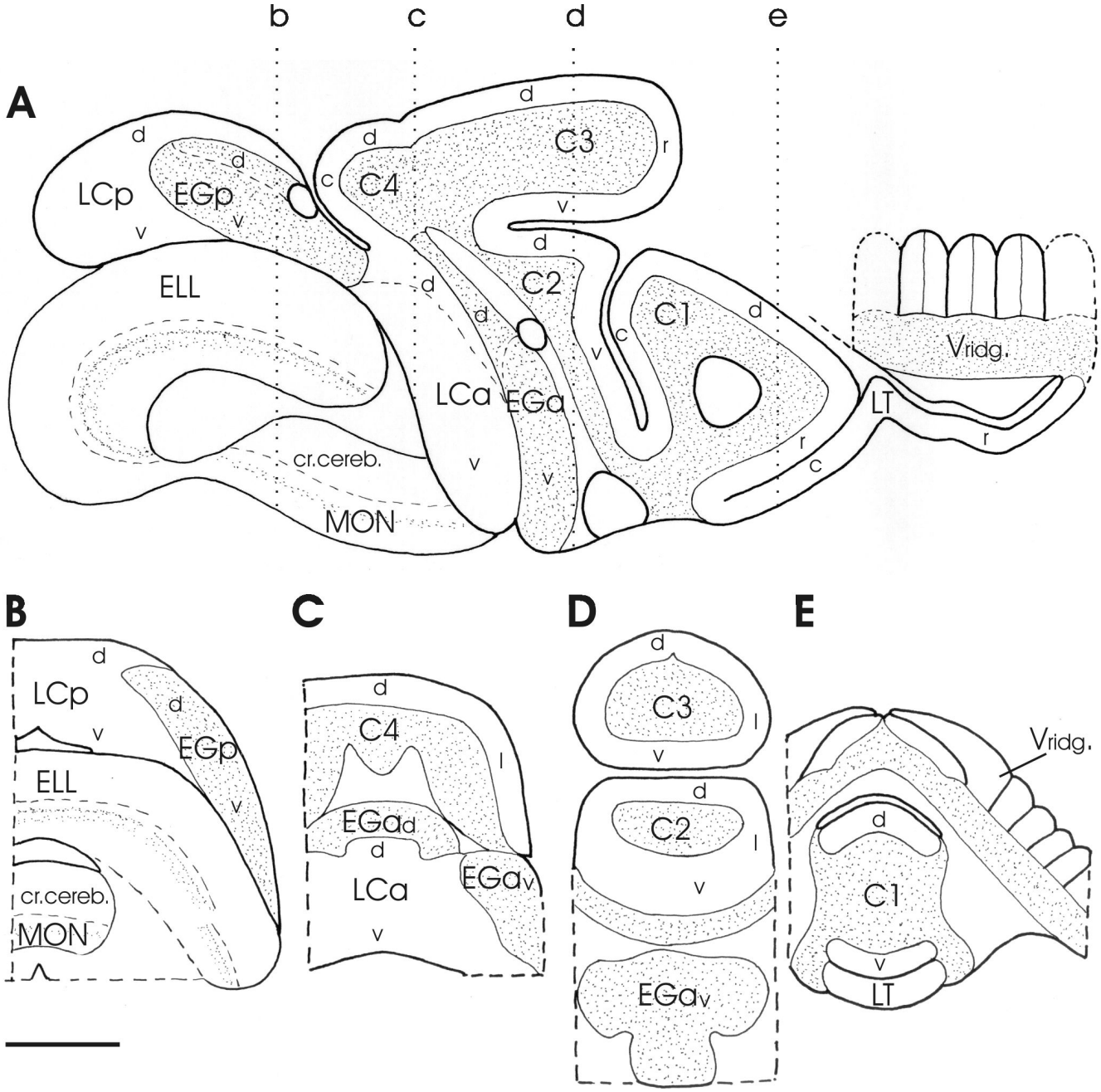

Fig. 3.

Schematic drawings of a parasagittal section (A) and four transverse sections (B-E) at levels indicated in a, showing the location and extension of the different cerebellar subdivisions and subregions distinguished in the present study. In a, only a few ridges have been draw schematically out of the large number that actually can be seen in parasagittal sections (cf. Fig. 1 of Shi et al. 2008). Scale bar = 1 mm. Abbreviations in this and following figures: see list of abbreviations.

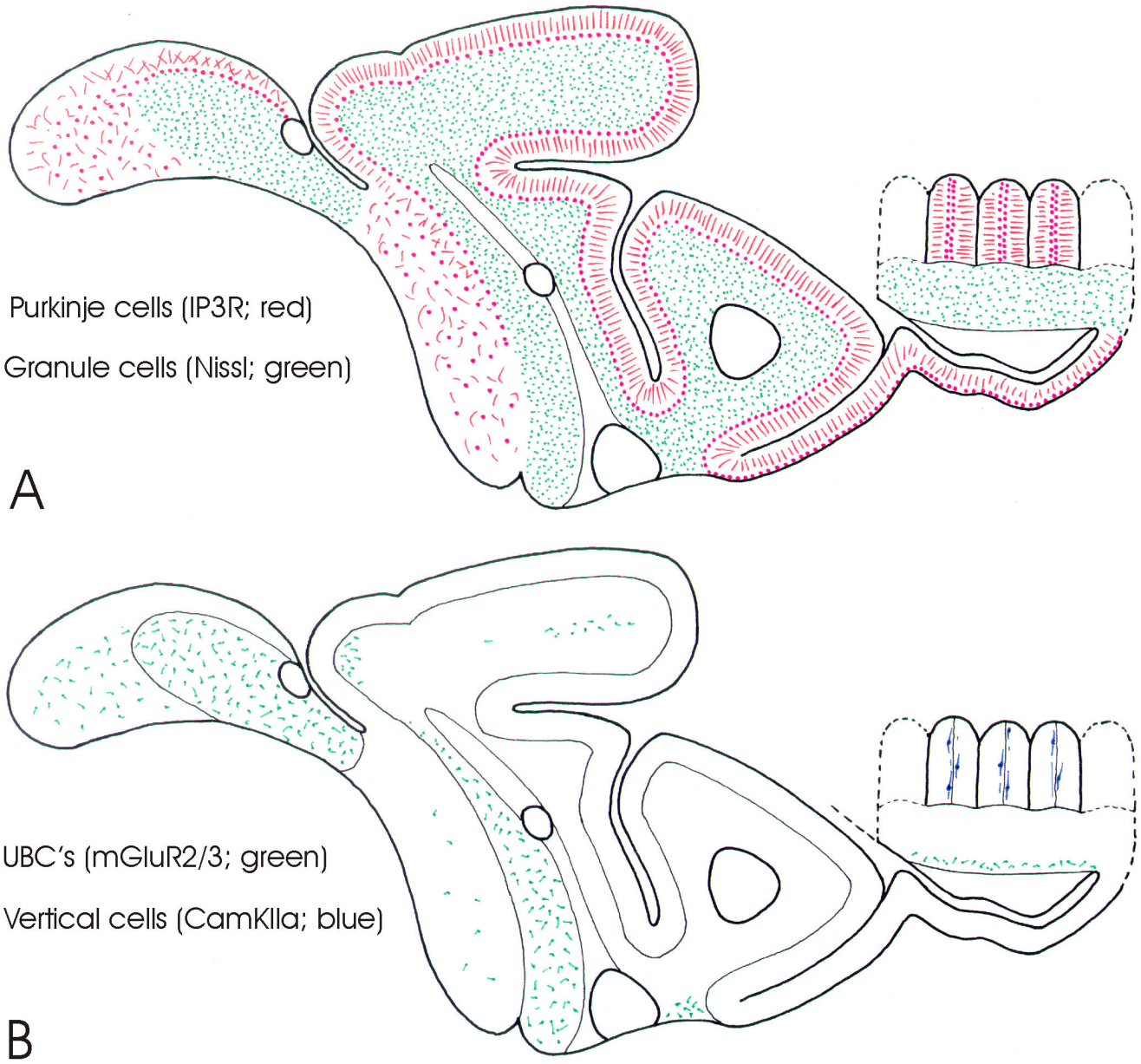

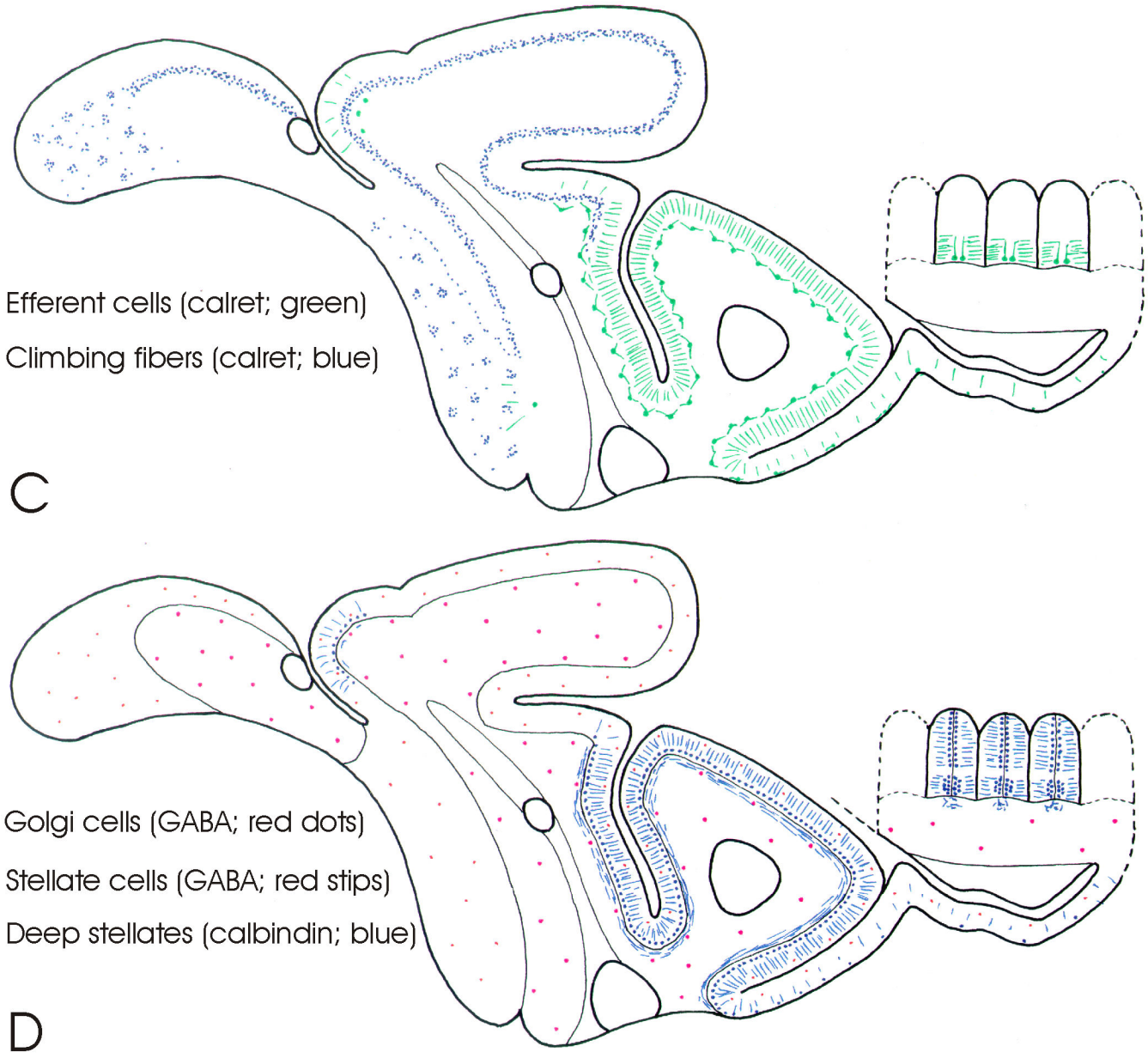

Fig. 4.

Schematic drawings of parasagittal sections through the cerebellum of *Gnathonemus petersii* (see Fig. 2 for subdivisions) showing overviews of the distribution of cerebellar neural elements as stained by different staining procedures and anti-bodies. **A:** The distribution of granule cells (green stipples), as shown in Nissl stains, and the distribution of the spiny dendrites (red lines) and cell bodies (red dots) of Purkinje cells, as shown by anti-IP3R staining. **B:** The distribution of unipolar brush cells (UBC's) and UBC-like cells (in green), as shown by anti-mGluR2/3, and the distribution of vertical cells (in blue), as shown by anti-CamKIIα staining. **C:** The distribution of climbing fiber terminals (blue stipples) in the corpus and caudal lobe, and of efferent cells in the valvula (in green) as shown by anti-

calretinin staining. **D:** The distribution of superficial stellate cells (red stipples) and Golgi cells (red dots) as shown by anti-GABA staining and the distribution of the axons, cells bodies as well as distal dendrites of deep stellate cells (in blue) as shown by anti-calretinin and anti-calbindin staining. Notice that not only superficial stellate cells and Golgi cells, but also deep stellate cells and Purkinje cells are GABA-positive, whereas efferent cells are glutamate-positive. We presume that climbing fibers, unipolar brush cells and granule cells, as in mammals, are glutamatergic as well, but this could not be ascertained in the present study.

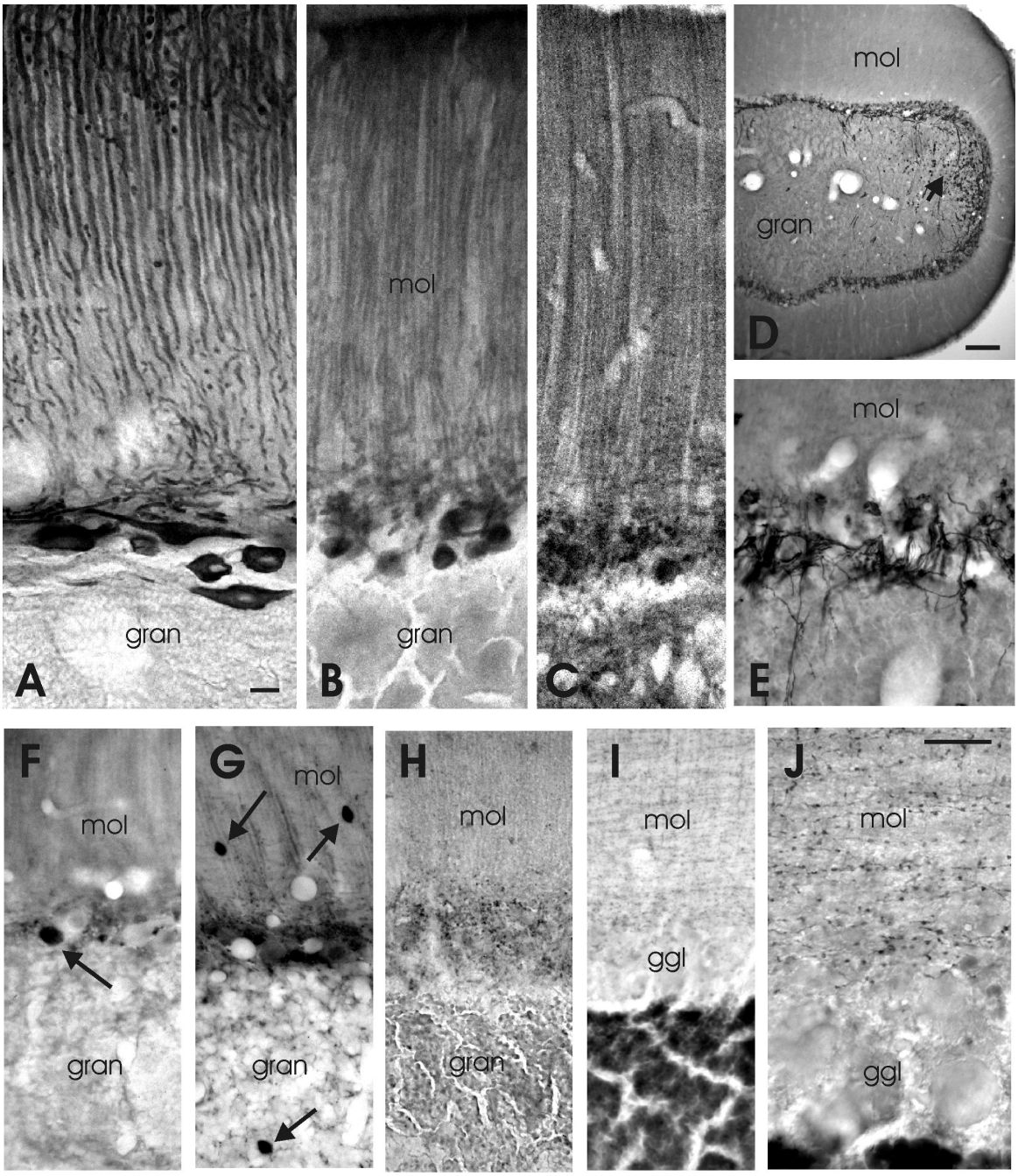

Fig. 5.

Photomicrographs of immunohistochemically stained sections of lobe C3 of the corpus cerebelli of *Gnathonemus petersii*. A is a sagittal section and E-J are transverse sections. **A:** Purkinje cells as stained with anti-IP3R. **B:** Purkinje cells as stained with anti-calcineurin. **C:** Purkinje cells as stained with anti-mGluR1α. **D:** Climbing fibers and UBC's as stained with caltetinin at low magnification; arrow points to the dorsolateral region where UBC's are present. **E:** Climbing fibers as stained with anti-calretinin at the same magnification as A-C. **F:** A presumed efferent cell as stained by anti-glutamate (arrow). **G:** A Golgi cell

(arrow in gran), stellate cells (arrows in mol) and fragments of Purkinje cells in the ganglionic layer, as stained with anti-GABA. **H:** The distribution of gephyrin-positive spots. **I,J:** the distribution of presumed stellate axons and their varicosities as stained with anti-GABA-transporter 1 at the same magnification as F-H (I) and at higher magnification (J). Scale bar = 10 μm in A (applies to A-C and E-I); 100μm in D; 10μm in J.

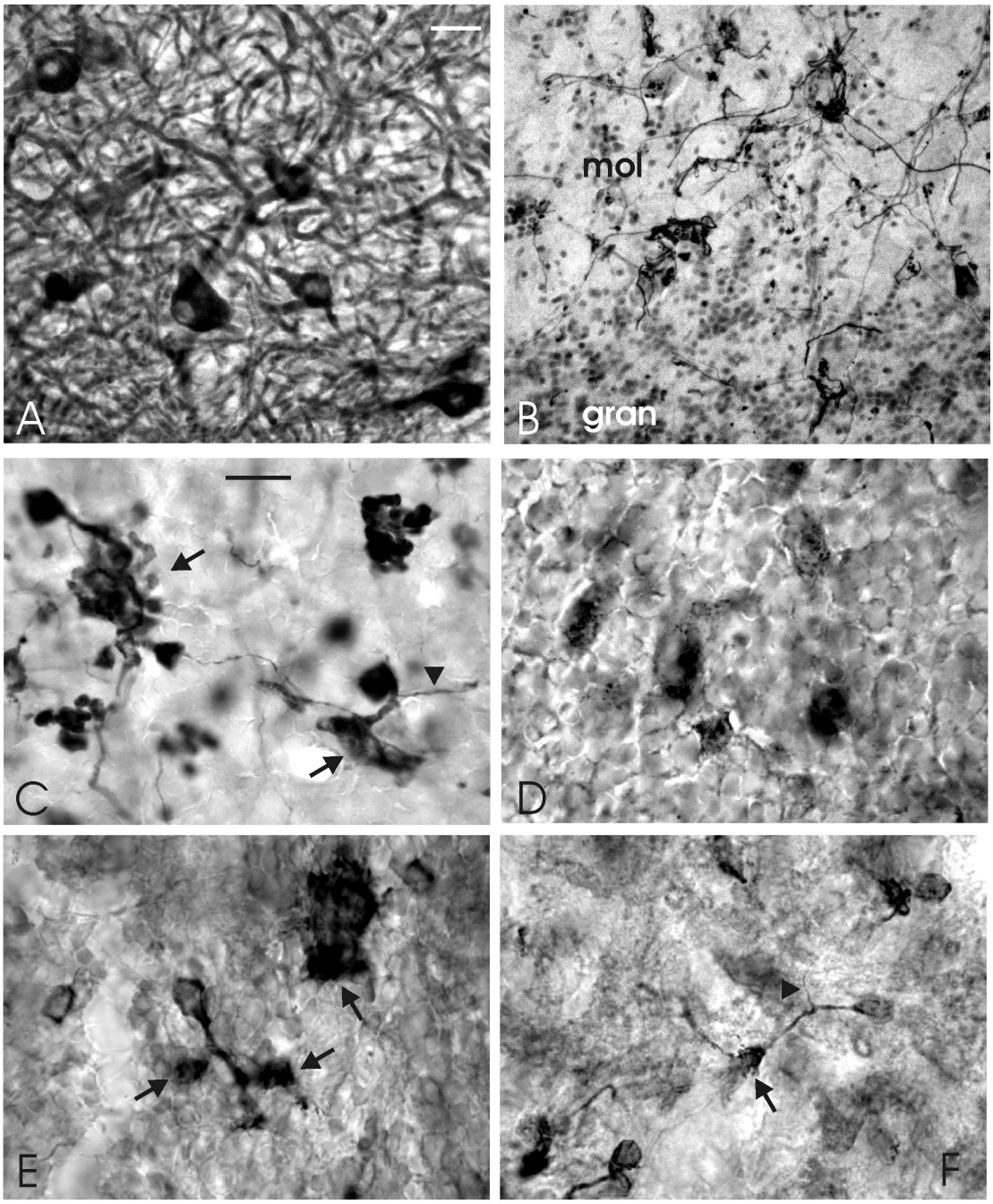

Fig. 6.

Photomicrographs of the most striking properties of the caudal cerebellar lobe of *Gnathonemus petersii* as shown with immunohistochemical techniques. **A:** The location of IP3R-positive Purkinje cells and their randomly oriented dendrites in the molecular layer of the posterior caudal lobe. **B:** The clustering of calretinin-positive climbing fiber terminals in the molecular layer around somata and proximal dendrites of Purkinje cells of the posterior caudal lobe. **C:** The staining of unipolar brush cells with anti-calretinin in the anterior granular eminence. **D:** The concentration of gephyrin-positive spots on certain larger

elements in the anterior granular eminence. **E:** The staining of unipolar brush cells (UBC's) in the posterior granular eminence with anti-GluR2/3. **F:** The staining of UBC-like cells in the molecular layer of the posterior caudal lobe. Arrows point to brushes of UBC's and arrowheads to their presumed axons. Scale bar = 20 μm in A (applies to A,B); 10 μm in C (applies to C-F).

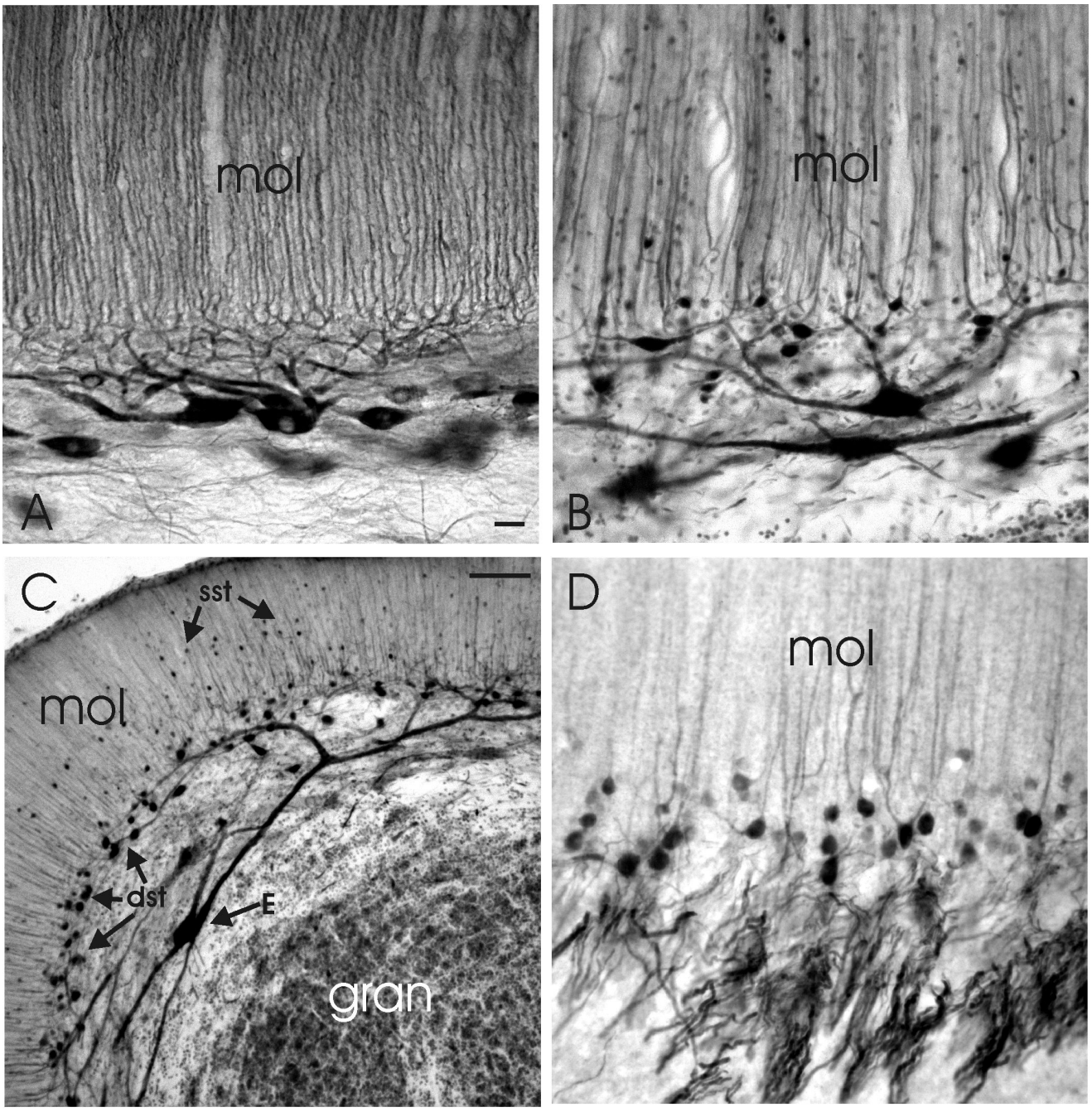

Fig. 7.

Photomicrographs of sagittal (A-C) and transverse sections (D) through lobe C1 of the proximal valvula. **A:** The properties of Purkinje cells as stained with anti-IP3R. **B:** The properties of efferent cells and deep stellate cells as stained with anti-calretinin. **C:** Low magnification of the properties of efferent cells and (superficial as well as deep) stellate cells as stained with anti-calretinin. **D:** The dendrites, cell bodies and axons of deep stellate cells as stained with anti-calbindin. Scale bar = 10μm in A (applies to A,B and D); 50 μm in C.

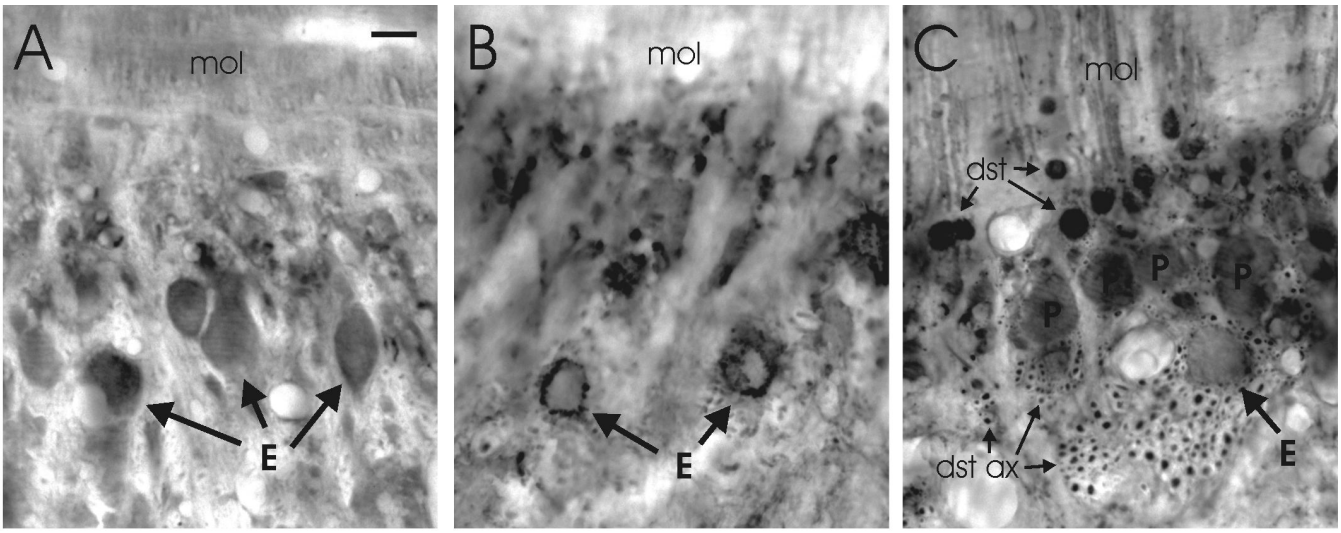

Fig. 8.

Photomicrographs of transverse sections through lobe C1 of the proximal valvula. **A:** The staining of efferent cells by anti-glutamate. **B:** The distribution of GAD-positive terminals. **C:** The distribution of GABA-positive structures, including the somata of deep stellate cells (dst) and Purkinje cells (P) and the sagitally oriented bundles of deep stellate axons (dst ax) between the layer of Purkinje cells and the granular layer. Scale bar = 10 μm.

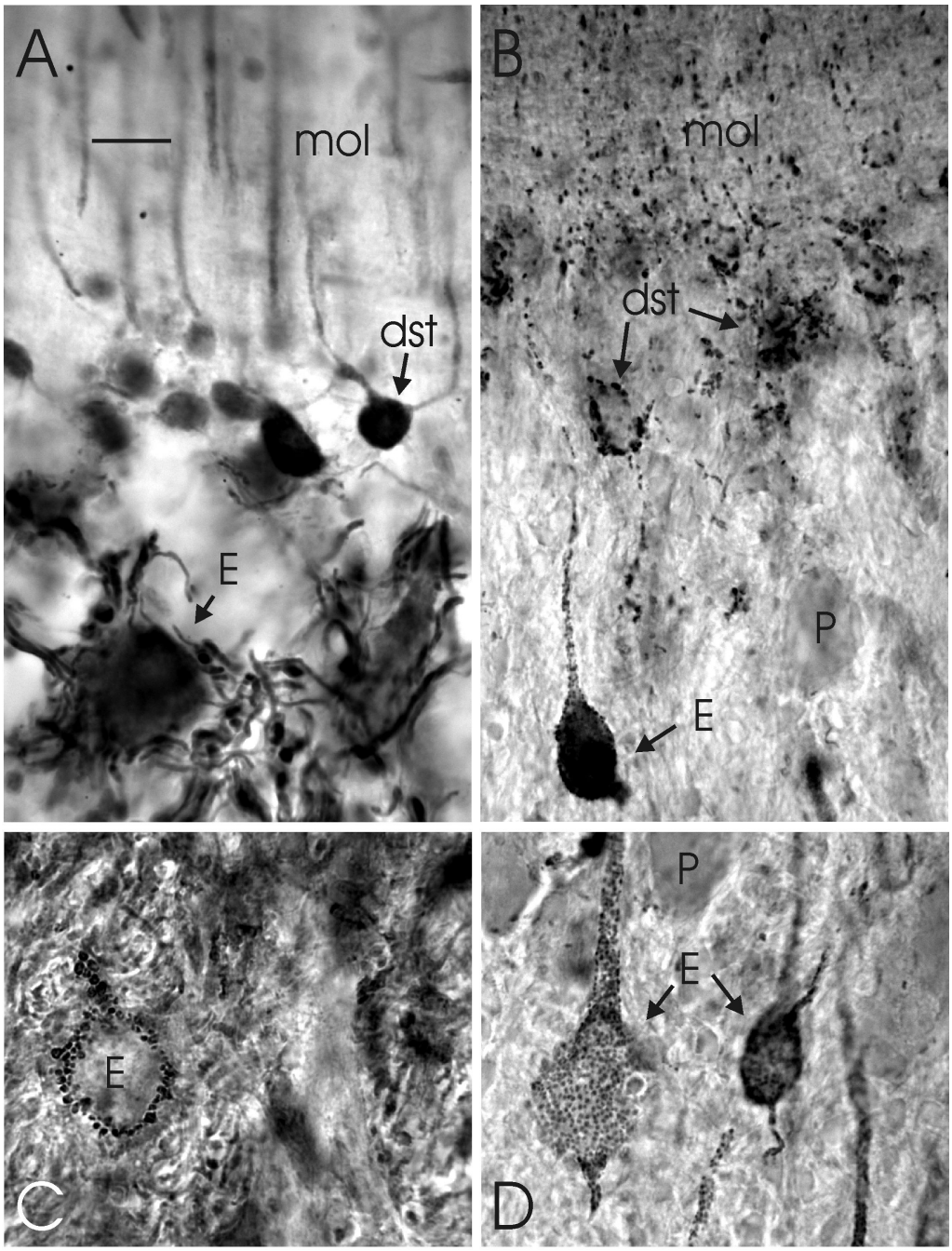

Fig. 9.

Photomicrographs of transverse sections showing details of the dense innervation of efferent cells by axon terminals of deep stellate cells in lobe C1 of the proximal valvula. **A:** The dense plexus of axons around an efferent cell body as stained with anti-calretinin. **B:** The distribution of gephyrin-positive spots, showing a special concentration on the cells bodies of an efferent cells and some deep stellate cells and a substantial density in the deep molecular layer. **C:** The high density of GAD-positive terminals around an efferent cell

body. **D:** The high density of gephyrin-positive spots on two efferent cell bodies. Scale bar = 10 μm (applies to A-D).

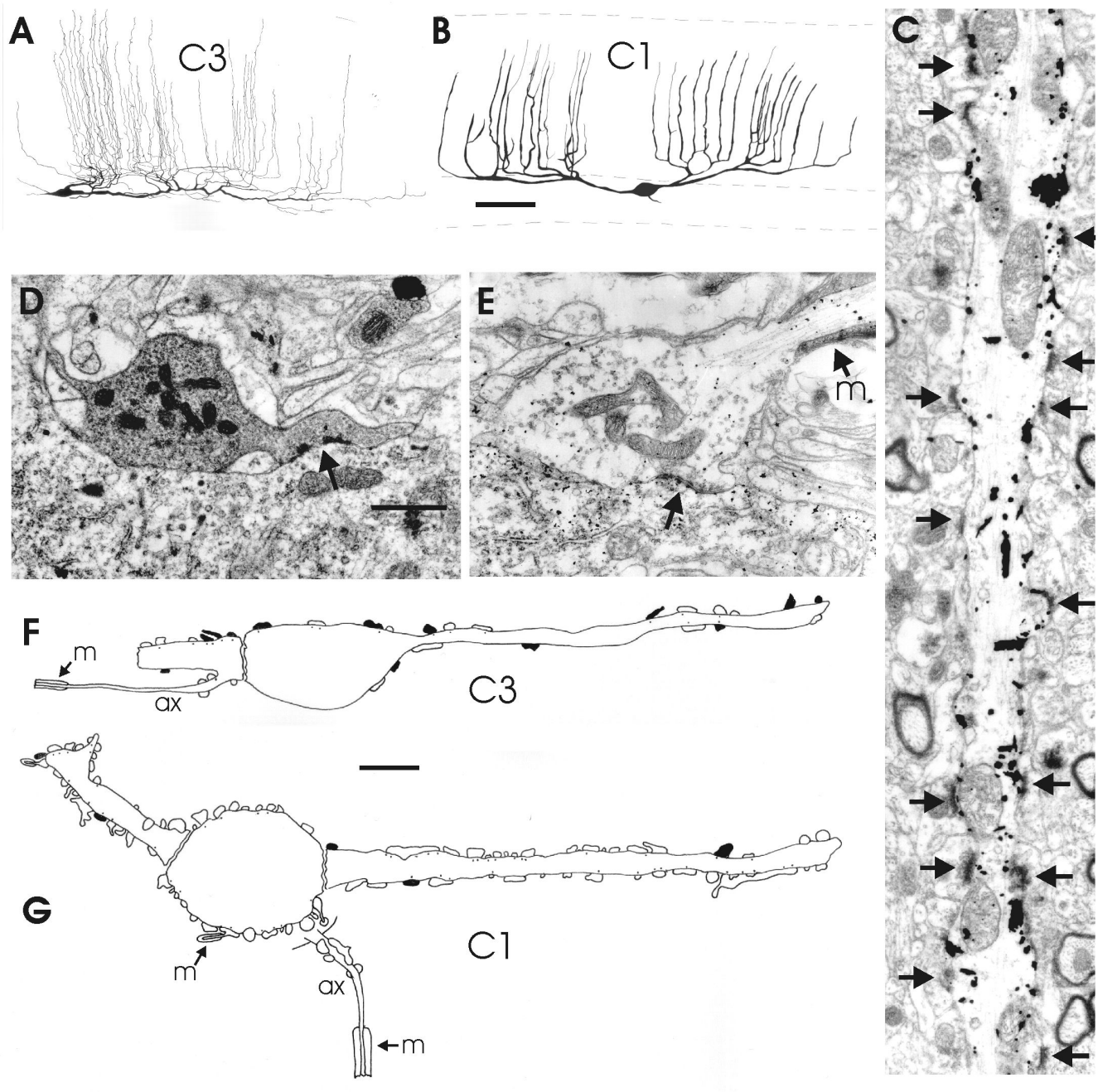

Fig. 10.

Morphological properties of efferent cerebellar cells in the corpus (lobe C3) and the proximal valvula (lobe C1) as shown by Golgi impregnation and electron microscopy. **A,B:** drawings of sagittal views of Golgi-impregnated efferent cells in lobe C3 (A) and C1 (B). **C:** Electron microscopical picture of a portion of an apical dendrite of a Golgi-impregnated efferent cell in lobe C1. **D,E:** Electron micrographs of a Purkinje axon terminal (D) and a deep stellate axon terminal (E) on efferent cells in lobe C1; the efferent cell in E is Golgi-deimpregnated. **F,G:** Composite drawings of the distribution of Purkinje axon terminals

(black) and (deep) stellate axonal terminals (white) on profiles of efferent cells in lobe C3 (F) and lobe C1 (G), as observed in the electron microscope. Arrows point to synaptic contacts. Scale bar = 50 μm in B (applies to A, B), 1 μm in D (applies to C-E); 5 μm in F,G.

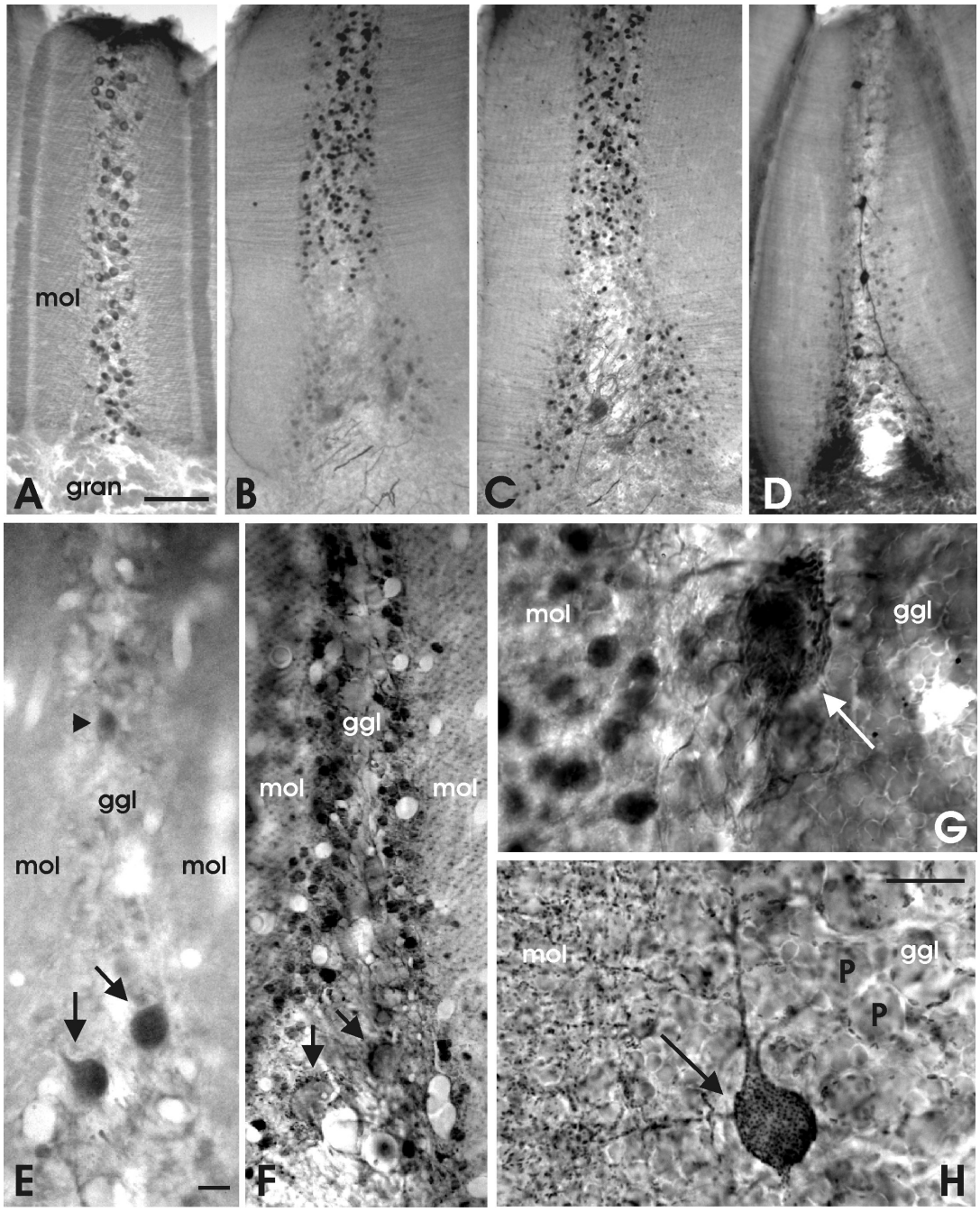

Fig. 11.

Photomicrographs of transverse sections through valvular ridges at low (A-D), intermediate (E,F) and high (G,H) magnification. **A:** The distribution of Purkinje cells as stained with anti IP3R. **B:** The distribution of deep stellate cells as stained with anti-calbindin. **C:** The distribution of deep stellate cells and basal efferent cells as stained with anti-calretinin. **D:** The distribution of vertical cells and some deep stellate cells as stained with anti-CAmKIIα. **E:** The staining of two basal cells (arrows) and a possible vertical cell (arrowhead) with anti-glutamate. **F:** The distribution of GABA-immunoreactivity. **G:** The high density of deep

stellate axons around a basal cell as stained with anti-calretinin. **H:** The distribution of gephyrin-positive synaptic spots in the proximal, basal part of a valvular ridge. Arrows point to basal cells. Scale bar = 50 μm in A (applies to A-D); 10 μm in E (applies to E,F); 10 μm in H (applies to G,H).

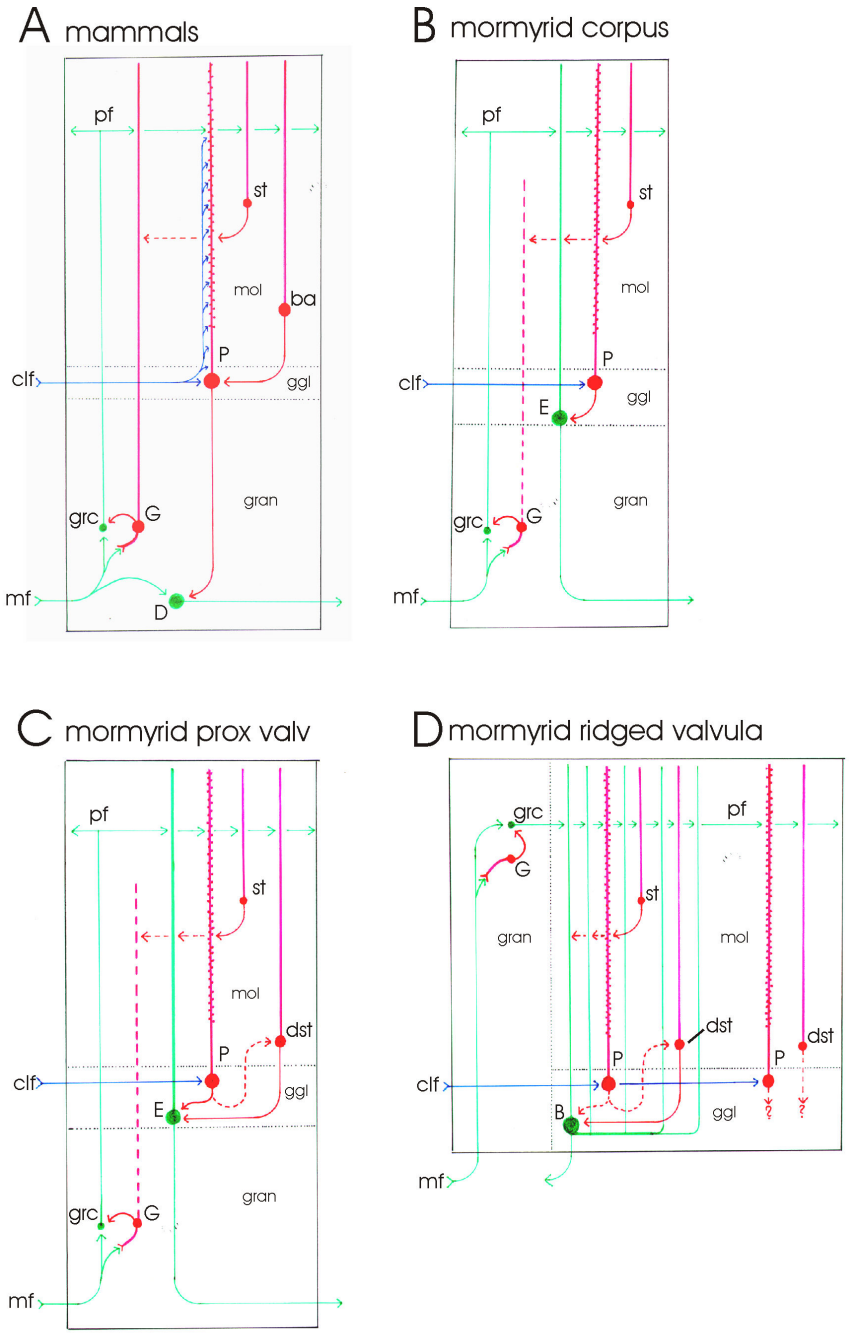

Fig. 12.

Schematic drawings of transverse views of cerebellar circuitry. **A:** Mammals. **B:** The mormyrid corpus cerebelli. **C:** The proximal valvula of mormyrids. **D:** The ridged valvula of mormyrids. For details, see the Discussion section.

J Comp Neurol. Author manuscript; available in PMC 2018 March 21.

Table 1

Summary of the mormyrid cerebellar elements stained by different antibodies

cell type →	**P**	**E**	**(deep)St**	**G**	**UBC$_{(like)}$**	**gr**	**ve**	**clf**	**mf**
↓ antibody ↓									
anti-IP3R	+								
anti-calcineurin *	+								
anti-mGluR1α	+								
anti-NR1 *		Vp,Vr	± in Vp,Vr					LC,Co	
anti-calretinin		Vp,Vr	Vp,Vr(subpop.)		EG,Co			LC,Co	EG
anti-calbindin		few in Vr		±	EG,Co				EG
anti-mGluR2/3					+				
anti-CamKIIα *	dendrites in Co		± in Vr (subpop.)				Vr		
anti-glutamate		Vp,Vr few in Co					few in Vr		
anti-GABA	±		+	+					

anti-GAD: terminals throughout the cerebellum, especially dense on E cells in Vp and Vr

anti-gephyrin: postsynaptic spots throughout the cerebellum, especially dense on E cells in Vp and Vr

anti-GAT1: fine terminal plexus in the molecular layer of all cerebellar subdivisions

Abbreviations in the upper row indicate cerebellar elements and abbreviations in the table indicate the cerebellar subdivisions in which dense staining was observed (or weak, when combined with ±). Abbreviations are explained in the list of abbreviations.

+ indicates dense staining in all cerebellar subdivisions.

± indicates weak staining in all cerebellar subdivisions.

* indicates antibodies for which the immunospecificity in the mormyrid brain is not certain